



UNIVERSITÀ  
DEGLI STUDI  
DI PADOVA

**Head Office: Università degli Studi di Padova**

**Department of Biology**

Ph.D. COURSE IN: Biosciences

CURRICULUM: Cell Biology and Physiology

SERIES XXX

***Helicobacter pylori* affects antigen presentation  
activity of macrophages modulating the expression of  
the immune receptor CD300E through miR-4270**

**Coordinator:** Prof. Ildikò Szabò

**Supervisor:** Prof. Marina de Bernard

**Ph.D. student:** Matteo Pagliari

# Table of contents

<b>1</b>	<b>Summary</b>	<b>4</b>
<b>2</b>	<b>Introduction</b>	<b>7</b>
2.1	<b>Helicobacter pylori</b>	<b>7</b>
2.2	<b>Epidemiology and transmission</b>	<b>8</b>
2.3	<b>Hp virulence factors</b>	<b>9</b>
2.3.1	Urease	9
2.3.2	Flagella and adhesins	10
2.3.3	CagPAI and the Type IV secretion system	10
2.3.4	Cytotoxin associated gene A (CagA)	11
2.3.5	Vacuolating cytotoxin A (VacA)	12
2.3.6	HP-NAP	14
2.3.7	Lipopolysaccharide (LPS)	15
2.4	<b>Hp associated diseases</b>	<b>16</b>
2.5	<b>Immune response to Hp and immune evasion mechanisms</b>	<b>17</b>
2.5.1	Macrophages in Hp infection	18
2.5.2	T lymphocytes in Hp infection	19
2.6	<b>Hp and miRNAs</b>	<b>21</b>
<b>3</b>	<b>Materials and methods</b>	<b>23</b>
3.1	<b>Monocytes isolation from buffy coat</b>	<b>23</b>
3.1.1	Differentiation of monocytes into macrophages	23
3.2	<b>Hp growth</b>	<b>23</b>
3.2.1	Growth on plate	24
3.2.2	Hp infection experiments	24
3.3	<b>Flow cytometry</b>	<b>25</b>
3.4	<b>Phagocytosis assay</b>	<b>27</b>
3.5	<b>Patients</b>	<b>27</b>
3.6	<b>Immunohistochemistry</b>	<b>28</b>
3.7	<b>Protein extraction from cells and protein quantification</b>	<b>28</b>
3.8	<b>Western blot</b>	<b>28</b>
3.9	<b>RNA extraction and gene expression analysis</b>	<b>29</b>
3.9.1	mRNA extraction	29
3.9.2	miRNA extraction	30

3.9.3	cDNA synthesis .....	30
3.9.4	Real-time PCR.....	30
<b>3.10</b>	<b>ELISA assay .....</b>	<b>33</b>
<b>3.11</b>	<b>Microarray expression profiles .....</b>	<b>33</b>
3.11.1	mRNA microarray .....	33
3.11.2	miRNA microarray.....	34
<b>3.12</b>	<b>Microarray data analysis.....</b>	<b>34</b>
3.12.1	mRNA microarray analysis.....	34
3.12.2	miRNA microarray analysis .....	35
<b>3.13</b>	<b>Luciferase assay.....</b>	<b>35</b>
3.13.1	Cloning of miRNA target expression vector .....	35
3.13.2	Luciferase assay .....	36
<b>3.14</b>	<b>Functional assay .....</b>	<b>38</b>
<b>3.15</b>	<b>Proliferation assay .....</b>	<b>39</b>
3.15.1	Generation of tetanus toxoid-specific cell clones.....	39
3.15.2	CSFE-based proliferation assay.....	39
<b>3.16</b>	<b>Statistical analysis .....</b>	<b>40</b>
<b>4</b>	<b>Results and discussion.....</b>	<b>41</b>
<b>4.1</b>	<b>Hp infection modulates miRNA expression in macrophages.....</b>	<b>41</b>
<b>4.2</b>	<b>Identification of miRNA targets.....</b>	<b>42</b>
<b>4.3</b>	<b>miR-4270 regulates the expression of <i>CD300E</i>.....</b>	<b>44</b>
<b>4.4</b>	<b>Hp-infected macrophages expose CD300E on the plasma membrane .....</b>	<b>45</b>
4.4.1	Hp infected macrophages express CD300E .....	45
4.4.2	Macrophages infected with Escherichia coli don't express CD300E .....	47
<b>4.5</b>	<b>Macrophages expressing CD300E infiltrate the mucosa of Hp-induced gastritis ..</b>	<b>47</b>
<b>4.6</b>	<b>CD300E activation effects on macrophages .....</b>	<b>49</b>
4.6.1	CD300E activation establishes a pro-inflammatory profile.....	49
4.6.2	CD300E activation affects antigen presentation.....	50
4.6.3	CD300E activation enhances phagocytosis.....	52
<b>5</b>	<b>Conclusions.....</b>	<b>55</b>
<b>6</b>	<b>Bibliography.....</b>	<b>57</b>

# 1 Summary

*Helicobacter pylori* (Hp) is a Gram-negative, microaerophilic, spiral-shaped bacterium that colonizes the gastric mucosa of almost half of the human population. In the majority of cases the infection remains asymptomatic, but in a small percentage of the infected people severe diseases may arise, such as peptic ulcer, chronic gastritis and gastric cancer. Despite the fact that the bacterium elicits a robust inflammatory and immune response, in absence of any antibiotic treatment, it can survive within the host for decades. This probably occurs because of its ability in modulating the host immune response, but this issue remains to be fully elucidated.

In the recent past it has been demonstrated that the infection by Hp is associated with the modulation of the expression of several miRNAs and abnormalities in miRNAs expression have been shown to be implicated in gastric cancerogenesis. However, the possibility that Hp modulates the expression of miRNAs also during the inflammation that precedes the development of cancerous lesions, was poorly considered.

Macrophages are the most abundant immune cells in the gastric mucosa of Hp-infected patients, thus their role in orchestrating the inflammation is expected to be crucial. Based on this consideration, in this study we investigated whether Hp modulates the inflammatory response in the gastric mucosa of infected patients by modulating the expression of miRNAs in macrophages.

Using a genome-wide approach, we analyzed the pattern of miRNAs expression in human monocytes-derived macrophages infected with Hp. We found that many miRNAs were modulated by the infection; since Hp infection triggers a chronic inflammation, we reasoned that down-regulated miRNAs, being permissive on the expression of their target genes, were the most interesting to investigate.

Taking advantage of an *in silico* analysis we predicted the human genes expected to be the targets of the modulated miRNAs and we confirmed by RT-PCR that those encoding proteins related to inflammation, such as the chemokines CCL2, CXCL6, and CCL22, FOXP4 and the immune receptor CD300E, were actually up-regulated in infected macrophages. Notably, the CD300E mRNA appeared as the most up-regulated mRNA in infected macrophages and it is target of one of the most down-regulated miRNA, namely has-miR-4270.

CD300E belongs to an emerging family of regulators of the immune system; it is an immune receptor expressed on the surface of monocytes. Although its ligand has not been identified yet, in monocytes the engagement of CD300E with an agonistic monoclonal antibody

stimulates the transcriptional activity of the nuclear factor of activated T cells and the release of reactive oxygen species. The engagement of the receptor also leads to the release of inflammatory cytokines and promotes the cell survival. The expression of CD300E decreases when monocytes differentiate into macrophages, thus we found interesting the evidence that macrophages infected by Hp got back the expression of the receptor.

We confirmed by TaqMan assay that miR-4270 is actually down-regulated in macrophages infected with Hp. The specificity of interaction between miRNA and its target has been further confirmed firstly by a luciferase-based assay and then by the evidence that the transfection of infected macrophages with a miR-4270 miRNA mimic dropped down the expression of CD300E on the surface of the cells.

By FACS analysis we confirmed that macrophages infected by the bacterium significantly increase the cell surface expression of CD300E, compared to uninfected cells; moving from cell-based assays to human-derived samples, we demonstrated that macrophages infiltrating the gastric mucosa of Hp infected patients suffering from gastritis, are enriched in CD300E. This part of the research revealed that the increased expression of CD300E in macrophages is linked to the presence of the bacterium, since its eradication is accompanied by the reduction of CD300-positive macrophages and no CD300E-expressing macrophages are present in gastritis caused by drugs (i.e. NSAID) as well as in the gastric mucosa of healthy donors. These results suggested that CD300E up-regulation could be considered a peculiarity of Hp infection; this idea was also corroborated by the observation that the exposure of macrophages to a non-pathogenic bacterium did not increase CD300E expression.

We revealed that the CD300E engagement by the agonistic antibody, elicited a pro-inflammatory profile in macrophages, as testified by the release of IL-1 $\beta$  and IL-6.

Notably, CD300E activation resulted also in the abatement of the major histocompatibility complex class II (MHC-II) dependent pathway of antigen presentation. In particular, we found that that mRNAs encoding for *HLA-DMA*, *HLA-DMB*, *HLA-DOA*, *HLA-DPA1*, *HLA-DPB*, *HLA-DRB1*, *HLA-DRB3*, *HLA-DRB4* and *HLA-DRB5* were strongly down-regulated.

These data were confirmed by the reduced exposure of the MHC-II molecules on the surface of macrophages exposed to the agonistic antibody; in particular, we evidenced a significant decrease in the HLA-DR expression on the surface of macrophages.

Such a decreased expression of HLA-DR resulted in the impairment of the antigen presentation ability to T lymphocytes, as revealed by a proliferation assay.

Taken together, our data add another piece to the complicate puzzle represented by the long-life coexistence between Hp and the human host, reinforcing the idea that Hp-infected

macrophages may have a pivotal role in the persistence of Hp in the host. Moreover, our study contributes with new insights towards understanding the regulation and function of the immune receptor CD300E.

## 2 Introduction

### 2.1 *Helicobacter pylori*

*Helicobacter pylori* (Hp) is a Gram-negative, microaerophilic, spiral-shaped bacterium, with a bundle of flagella, which confers it motility (Figure 1).

It was firstly described in 1893 by Giulio Bizzozero, who noticed the presence of some spiral-shaped bacteria in dogs' stomach. However almost a century was needed in order to have the bacterium isolated and cultured, in 1983, thanks to Marshall and Warren who were able to correlate its presence into the stomach with gastric disorders [1]. This discovery made the two scientists worthy for the Nobel Prize in medicine in 2005.

The ability to colonize human stomach surviving in an extremely acid environment makes Hp one of the most successful human bacterial parasites, giving end to the paradigm that the stomach is a sterile niche.

Hp has infected humans for more than 58000 years and this long-term association has resulted in a phylogeographic distribution pattern of the bacterium that is shared with its host. Thus, the bacterium has been used as a tool for tracing demographic events and in human prehistory, sometimes also rewriting the chronology of human migration [2] [3].

Today it is reported to infect almost half of the population; however, despite its extremely high prevalence, only a little percentage of the infected people has clinical consequences, developing Hp-related diseases.

The infection can evolve to chronic, atrophic, and eventually autoimmune gastritis, peptic ulcer, mucosa associated lymphoid tissue (MALT) lymphoma and gastric adenocarcinoma. Due to the strong association between Hp infection and the increased risk in developing adenocarcinoma, the bacterium has been included in class 1 category of carcinogens by the International Agency for Research on Cancer (IARC) in 1994 [4].

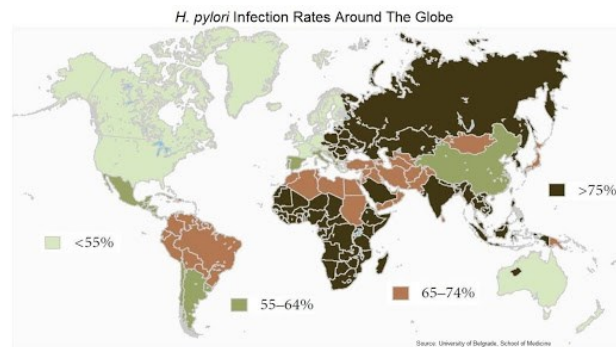


Figure 1: *Helicobacter pylori*. Image from [www.ebi.ac.uk](http://www.ebi.ac.uk)

## 2.2 Epidemiology and transmission

*Hp* infects the gastric mucosa of more than half of the human population and it is almost ubiquitous worldwide. In 2015 it was estimated that 4.4 billion people were infected [5].

There are many factors that contribute to the spreading of this pathogen. Socioeconomic conditions have a great impact on the incidence of *Hp* infection: in highly industrialized country, with better living condition, the prevalence of *Hp* has been declining (less than 50% of the population is infected); on the contrary, incidence is still at high levels in developing countries (more than 70%) (Figure 2), according with different levels of urbanization, sanitation, hygiene practices. Also bacterial factors, as well as host characteristics, affect the diffusion of *Hp*; it is reported, for example, that even ethnical differences or age may contribute to the differential infection rate among populations [6].



**Figure 2:** The picture shows the different prevalence rate of *Hp* infection in developing and developed country. Image from [www.bionap.whotrades.com](http://www.bionap.whotrades.com)

The mechanisms of transmission are still incompletely characterized. Person to person transmission is most commonly implicated, through faecal/oral, oral/oral and gastric/oral pathways. The bacterium has been isolated from saliva, vomitus and stools, suggesting that the organism is potentially transmissible during episodes of gastrointestinal tract illness [7]. It is worth of notice that recently some studies have been published with the hypothesis that *Hp* transmission would occur through contaminated water or food [8].

Infection usually occurs during the childhood and, without proper antibiotic treatment, the bacterium persists within the host for his entire lifetime. In the majority of cases the inflammatory state elicited by *Hp* remains sub-clinical and its detection is reached only by immunohistochemical analysis; however, about 15-20% of infected patients develop gastric disorders. The development of different gastric diseases depends on the host immune response, but also on the bacterial strain or environmental factors [9].



## **2.3 Hp virulence factors**

Hp produces a huge number of virulence factors that allow it to survive in the stomach, bind to epithelial cells, resist to phagocytosis and cause severe damage and inflammation. These factors include: urease, an enzyme essential for the survival of the bacterium in the gastric lumen, by producing ammonia that buffers the pH; flagella, which make the bacterium able to swim through the mucus layer; the *cag* pathogenicity island *cagPAI*, a genetic unit which encodes for the type IV secretion apparatus and inject the cytotoxin associated gene A (*CagA*) into gastric epithelial cells; *VacA*, a vacuolating cytotoxin capable also to impair the immune response; HP-NAP, a pro-inflammatory protein which promotes Th1 inflammation.

### **2.3.1 Urease**

One of the main adaptive features of Hp is the ability to survive in an extremely hostile environment such as that of the stomach. With its acidic pH, that ranges around 1 or 2, the gastric lumen prevents the survival of the majority of microorganisms. Urease allows Hp to survive in the stomach buffering the pH near the bacterial surface.

The expression of urease is regulated by a cluster of genes composed of seven genes, which includes those encoding the catalytic subunits *ureA* and *ureB*, an acid-gated urea channel and accessory proteins.  $\text{Ni}^{2+}$  is required by the enzyme to fold correctly in a dodecamer, formed by six units of *UreA* and six units of *UreB* [10]. The enzyme localizes in the cytosol of the bacterium and its activity is regulated by the proton-gated urea channel that allows urea entry only under acidic condition in order to prevent lethal alkalinisation. Once in the cytosol, urea is hydrolysed into  $\text{NH}_3$  and  $\text{CO}_2$ . Ammonium is extruded across the inner membrane, allowing rapid neutralization of protons entering the periplasm and, more important, create a neutral layer around the bacterial surface [11]. Urease is found also on the Hp surface: it is released by lysed bacteria and binds to the membrane of living Hp where produces ammonium to increase the buffering of pH [12].

Interestingly, mucosal viscosity is highly dependent on acidity, with mucus more viscous in a more acidic pH. Consistent with this notion, urease activity provides an opportunity for Hp to penetrate deeply into the mucus, avoiding the acidic conditions in the middle of the lumen and reaching a more viable niche.

Finally, urease activity is used to diagnose the presence of Hp. Patients ingest  $^{13}\text{C}$ - or  $^{14}\text{C}$ -labelled urea: if Hp is present in the stomach, labelled urea is hydrolysed in ammonium and  $\text{CO}_2$ ; the latter, containing the isotope, can be detected in patients' breath [13].

### **2.3.2 Flagella and adhesins**

Hp moves through the mucus layer thanks to a unipolar bundle of two to six flagella. These flagella are mainly composed of the basal body, hook and flagellar filament.

The basal body is formed by several structural proteins and it plays a role in providing the energy source for motility. The flagellar filament consists of two flagellins, FlaA and FlaB, encoded by *flaA* and *flaB*; both genes are essential for the motility of the bacterium and consequently for its ability to colonize the gastric epithelium. The hook links the basal body to the flagellar filament [14][15].

Once Hp reaches the epithelium, it can strongly adhere to gastric epithelial cells. This interaction is mediated by a group of proteins called adhesins. The best characterized adhesins are the blood-antigen binding protein A (BabA), that binds to Lewis b antigen on gastric epithelial cells, and the sialic acid-binding adhesion (SabA), that binds to sialylated-glycoconjugates antigen. Not all Hp strains express these adhesins; it is reported that BabA contributes to an increased risk of developing peptic ulcer and gastric cancer, whereas SabA is related to chronicization of the infection and to gastric atrophy and cancer [16][17].

### **2.3.3 CagPAI and the Type IV secretion system**

The *cag* pathogenicity island (cagPAI) is a 40 kb genetic locus that contains 27-31 genes, including *cagA*, which encodes proteins forming a type IV secretion system (T4SS), the molecular syringe by which the bacterium injects the cytotoxin CagA in the cytosol of gastric epithelial cells [18]. In addition, T4SS is able to promote IL-8 release by epithelial cells [19], thus contributing to the recruitment of neutrophils in the infected mucosa.

The presence of this locus discriminates highly virulent cagPAI-positive (type 1) from less virulent cagPAI-negative (type 2) strains. The cagPAI was acquired by a single horizontal DNA transfer event and it is remained almost unchanged over time, indicating that this acquisition resulted in an evolutionary advantage for the bacterium [20].

The T4SS is similar to the conjugation pilus present in other bacteria, and it is used by other pathogens, like *Bordetella pertussis* or *Legionella pneumophila*, to deliver virulence

molecules into infected host cells. In case of Hp, CagA is the only effector protein known being injected by T4SS [21].

According to a recent model proposed, CagL, one of the structural proteins located on the tip of the Hp T4SS, binds to  $\alpha_5\beta_1$  integrin (expressed by gastric epithelial cells) through an arginine-glycine-aspartate (RGD) motif providing one of the initial signals for the secretion of CagA. The surface located CagA binds to phosphatidyleserine (PS) on the host membrane. Binding of CagY and CagI to  $\beta_1$  integrin could further stabilise the interaction among the Hp T4SS, CagA and integrin, subsequently promoting the internalisation of PS-bound CagA through activation of integrin signalling (Figure 3) [21][22].

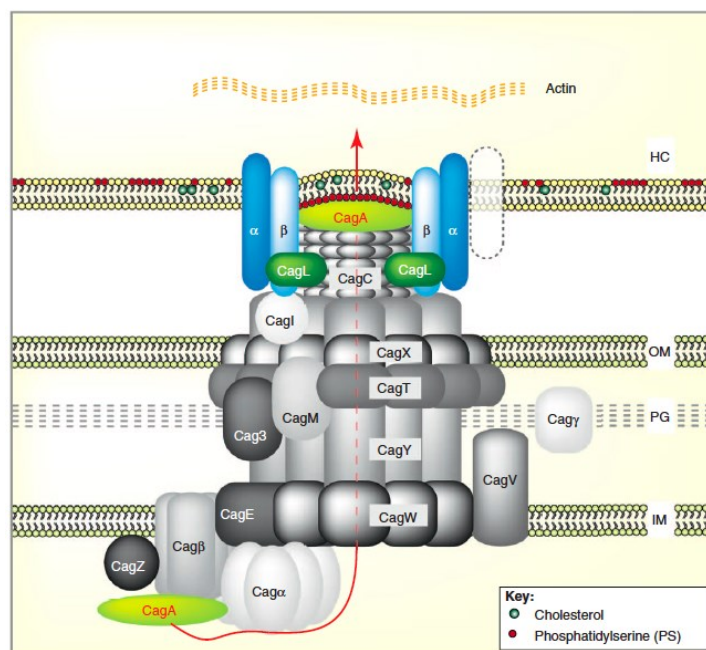


**Figure 3: Components of the T4SS and putative mechanism of CagA translocation. The host cytoplasm (HC), the bacterial outer membrane (OM), the layer of peptidoglycan (PG), and the bacterial inner membrane (IM) are indicated. Image adapted from [21]**

### 2.3.4 Cytotoxin associated gene A (CagA)

CagA is one of the best studied virulence factors and it is the first identified bacterial protein involved in human cancer. CagA is a 128 kDa protein that is injected directly from the bacterium inside the host cell through the T4SS. The protein has a tyrosine phosphorylation site which includes a highly conserved sequence of amino acids at the carboxyl terminal of the protein, Glu-Pro-Ile-Tyr-Ala, abbreviated to EPIYA [23][24]. Differences in the flanking regions of this sequence define the type of CagA, that can have different affinity for host

proteins resulting in various effects within the cells, with certain EPIYA polymorphisms that are more strongly associated with cancer than others [25].

After intracellular translocation, CagA can interact with several proteins in a tyrosine-phosphorylated-dependent or independent manner.

CagA is phosphorylated by host Src family protein tyrosine kinases [24]; in this phosphorylated form it binds to the phosphatase SHP-2 causing cytoskeleton rearrangements, increasing cell size, promoting elongation, thus affecting cells adhesion, spreading and migration [26]. Phosphorylated-independent activities of CagA are responsible for the disruption of cell-to-cell junctions and for triggering inflammation. CagA can affect cell-to-cell junctions of epithelial cells by interacting with an essential scaffold protein at the tight junctions, the zona occludens-1 (ZO-1), and with the junctional adhesion molecule JAM causing alterations in the cellular polarization and of junction-mediated functions [27]. In addition, CagA can interact with E-cadherin causing the disruption of adherence junctions in polarized epithelial cells, as well as the accumulation of  $\beta$ -catenin in the cytoplasm and nuclear sites, that leads to the activation of the so called Wnt signalling pathway which is involved in proliferation and regeneration of epithelial cells [28].

Collectively, these features support the notion that CagA may have a role in carcinogenesis; in accordance, it has been demonstrated that infections by *cagA*<sup>+</sup> strains are more frequently associated with gastric cancer, than *cagA*<sup>-</sup> strains [19].

### **2.3.5 Vacuolating cytotoxin A (VacA)**

The vacuolating cytotoxin A (VacA) is one of the major virulence factors secreted by Hp. Its name refers to the ability of inducing vacuoles in the cytoplasm of cells in culture [29]. It is initially synthesized as a polypeptide of 140 kDa and it is composed by a signal sequence, a passenger domain and an auto-transporter domain. The passenger domain contains the 33 KDa (p33) and the 55 KDa (p55) domains, that are processed and cleaved from the auto-transporter domain to form the mature 88 KDa VacA toxin [30].

All the Hp strains possess the VacA gene, however, there is a great variability due to polymorphisms along the sequence. These polymorphisms impact on the bacterium ability of causing severe diseases [31].

The monomeric VacA has a tendency to insert into membranes where it forms exameric oligomers that function as ion-permeable pores. The receptors implicated in the binding of the toxin to gastric epithelial cells include the epidermal grow factor (EGF) receptor,

glycosphingolipids and the receptor protein tyrosine phosphatase (RPTP) alpha and beta [32][33][34]. Once VacA is inserted into the plasma membrane of host cells, it is endocytosed and transported to endosomes/lysosomes. Here, the channels formed by the toxin facilitate the transport of chloride anions, resulting in an increase in intra-luminal chloride concentration and in the stimulation of the proton pump V-ATPase that is responsible for the acidification of the organelles; ultimately, membrane-permeable weak bases diffuse into these endocytic compartments where they become protonated and accumulate inside the endosomes. H<sub>2</sub>O enters in the endosomal lumen for osmosis, resulting in swelling and vacuolation [29][35].

Vacuolation is perhaps the most characteristic effect of VacA, but in the past decades it has been evidenced that VacA has a variety of effects on host cells in addition to the vacuole formation ability (Figure 4).

Indeed, VacA has been shown to localize to mitochondria from where it triggers the apoptotic cascade. It is still unclear the exact mechanism through which VacA would exert this role; however, evidence suggest that VacA forms membrane embedded pores in the inner mitochondrial membrane leading to the dissipation of the mitochondrial electrochemical membrane potential and the release of cytochrome c [36][37].

Interestingly, VacA can exert also both pro-inflammatory and anti-inflammatory activity.

It induces the release of pro-inflammatory cytokine (i.e. IL-8, IL-6, TNF- $\alpha$ , IL-1 $\beta$ ) by both epithelial and myeloid cells [38]. On the other hand, it is reported that VacA inhibits antigen-processing by Antigen Presenting Cells (APC) by interfering with late endocytic membrane trafficking. Indeed, the toxin interferes with proteolytic processing of antigens and the generation of T cell epitopes loaded on newly synthesized major histocompatibility complex class II (MHC-II) [64]. Accordingly, VacA-specific CD4<sup>+</sup> T-cells are found at low frequency in the gastric mucosa of infected patients [39]. This aspect will be described more in detail below.

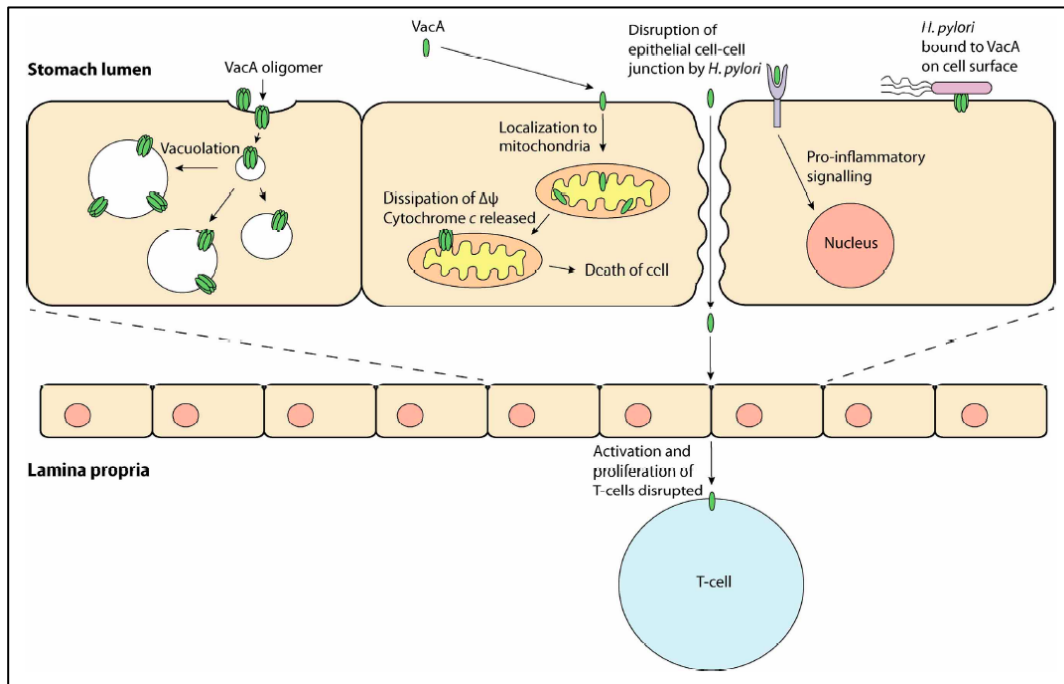


**Figure 4: Different VacA activities: the toxin may produce vacuoles, localize to the mitochondria inducing apoptosis, bind to cells inducing inflammation, or impair T-cell activation and proliferation. Figure adapted from [31].**

### 2.3.6 HP-NAP

The Hp neutrophil-activating protein (HP-NAP) is highly conserved among many isolates of Hp. It was firstly discovered in the bacteria supernatant as a protein that stimulated neutrophils to produce oxygen radicals. In addition to this, now it is clear that HP-NAP has a more complex role, being responsible of a variety of effects on the immune system. Indeed HP-NAP is now considered a crucial factor in driving the Th1 inflammation, a hallmark of Hp infection [40].

Structurally, the protein is a ball-shaped dodecamer, formed by the assembling of monomers of 17 kDa [41]. HP-NAP is likely released after cell lysis and it is able to cross the gastric epithelial layer reaching the underlying tissues where it encounters and activates the resident immune cells, such as mast cells and macrophages. Once accumulated in the tissues, HP-NAP recruits monocytes, neutrophils and lymphocytes, thus amplifying the inflammatory process. HP-NAP crosses the endothelium and from the luminal side it directly stimulates leukocytes to adhere and to extravasate [42].

Furthermore, HP-NAP stimulates monocytes and dendritic cells to express and release the pro-Th1 cytokines IL-12 and IL-23. In accordance, HP-NAP promotes the polarization of T lymphocytes towards the Th1 profile [40] (Figure 5).

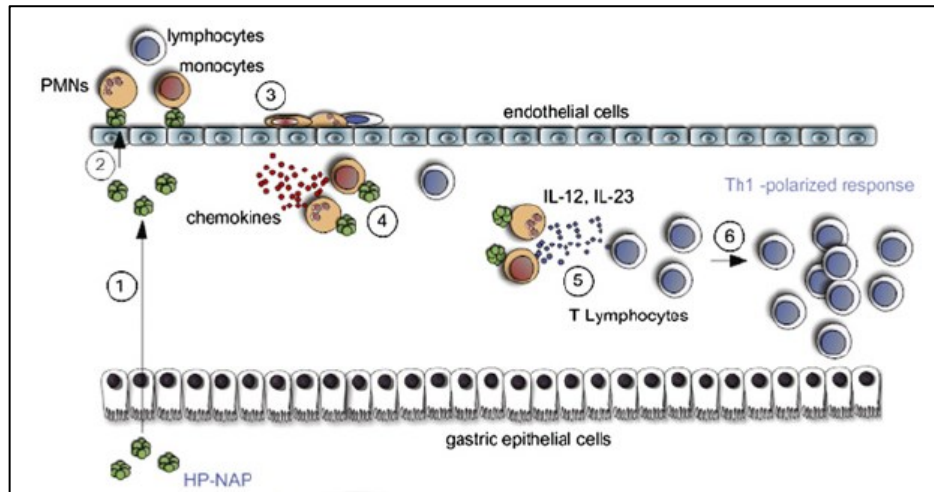


Figure 5: Model illustrating the role of HP-NAP in triggering the flogistic process associated to Hp infection and its immunomodulating activity. HP-NAP, once released by Hp, crosses the gastric epithelial lining (1) and the endothelium (2), and stimulates leukocytes to adhere and to extravasate (3). HP-NAP also activates neutrophils and monocytes to secrete chemokines (4). Furthermore, the protein is able to create a IL-12/IL-23 enriched milieu (5) which is responsible for driving the differentiation of T helper cells toward Th1 phenotype (6). Image adapted from [42]

### 2.3.7 Lipopolysaccharide (LPS)

The Hp LPS has the same basic structure of other Gram-negative LPS: a hydrophobic domain, embedded in the outer membrane, termed lipid A, that interacts with immune receptors and confers the LPS molecule with a range of immunological and potential toxic properties; a relatively conserved non-repeating core oligosaccharide, which influences permeation properties of the outer membrane; and a variable outermost polysaccharide named O-antigen, which contributes to the antigenicity and defines the serospecificity of the molecule. Compared to that of other Gram-negative bacteria, Hp LPS displays a very weak endotoxic activity (up to 1000-fold lower) [43].

The characteristic feature of Hp LPS is the presence on the O-antigen of Lewis blood group, very similar to those expressed by gastric epithelial cells [44]. This similarity to “self” antigen may represent a form of molecular mimicry or immune tolerance that enables Hp LPS to be shielded from immune recognition.

Furthermore, Hp Lewis blood group can interact with the C-type lectin DC-SIGN (Dendritic Cell Specific Intracellular adhesion molecule-3-Grabbing Non-Integrin) on dendritic cells to block the development of Th1, thus down-regulating the inflammatory response [45].

## **2.4 Hp associated diseases**

Hp infection is one of the most common bacterial infection worldwide and virtually all the infected people develop chronic active gastritis [46]. In the majority of cases, infected people live without knowing about the bacterial persistence into their stomach; however, a relevant percentage of infected subjects develops more severe diseases during the course of infection. If not properly treated, Hp infection and the related inflammation may become chronic leading, after decades, to peptic ulcer, autoimmune gastritis, gastric MALT lymphoma and gastric adenocarcinoma.

The mechanism of infection by the bacterium is predisposing to ulcer development: indeed, the inflammation elicited in the stomach stimulates G cells to release gastrin, a hormone that increases secretion of histamine. Histamine stimulates parietal cells to produce acid. The constant stimulation of parietal cells causes an increase in the acid production, which leads to the irritation of the mucous membrane. If the acid load doesn't decrease the situation may evolve into an ulcer [47].

Autoimmune gastritis is characterized by autoimmune-mediated destruction of gastric glands in the stomach. Hp-related induction of autoantibodies reactive with gastric mucosal antigens is thought to be related to the molecular mimicry between some Hp antigens and host molecules (i.e. Lewis blood group antigens on Hp LPS) [48]. Th17 lymphocytes are believed to contribute to the autoimmune gastritis [49].

The involvement of Hp in the development of MALT lymphoma is supported by the evidence that almost all patients are infected by the bacterium and that the eradication of the bacterium leads to remission in about 80% of them [50]. Some data indicate that the release of IL-2 following an immune response to Hp is involved in the development of the lymphoma [51]; others identify a proliferation inducing ligand (APRIL) produced by macrophages as an important factor for MALT development [52].

Finally, regarding gastric adenocarcinoma, it is established that Hp infection is the major risk for its development. Gastric adenocarcinoma is one of the most common forms of cancer and a leading cause of cancer-related deaths in several countries, killing more than 700000 people every year. Also in this case, many studies correlate the presence of the bacterium with the cancer development demonstrating that there is a decreased probability of gastric cancer development after a successful antibiotic therapy against Hp [53].



## **2.5 Immune response to Hp and immune evasion mechanisms**

Hp infection elicits inflammation in the gastric mucosa. The fact that the bacterium remains in the stomach at a high density and the persistence of inflammation for many years, support the notion that the immune response is dysregulated and somehow ineffective.

Both innate and adaptive immunity are involved in the response against Hp.

The innate immunity is the “first line of defence” in response to pathogens, and it does not require previous exposure to the immune stimulus. It is based on the action of several cell types such as monocytes, macrophages, dendritic cells (DC) and neutrophils, that rapidly establish an effective immune response against a pathogen. The main mechanisms to face the infection are the secretion of pro-inflammatory cytokines, phagocytosis, production of ROS or NO. Moreover, macrophages and DC have the role of presenting antigens to T cells, thus stimulating the adaptive response.

The adaptive immunity creates immunological memory after an initial response to a specific pathogen, and leads to an enhanced response to subsequent encounters with that pathogen.. In this case the immune response is extremely specific and it can be divided into humoral and cell-mediated response, depending on what type of cells is recruited: the humoral response is characterized by immunoglobulin production by B lymphocytes, while in the cell-mediated response, T cells directly secrete IFN- $\gamma$  that activates the killing potential of macrophages in order to kill the pathogen.

Despite the fact that Hp is considered a non-invasive pathogen because most of the bacteria reside in the mucus layer of the stomach in contact with the epithelium, it has been evidenced that the bacterium and its products can reach also the lamina propria and come in direct contact with immune cells within it [54]. Here, the bacterium induces a great influx of immune cells and it can be phagocytized by resident macrophages or by monocytes and neutrophils constantly recruited in inflamed gastric mucosa [55] (Figure 6).

The activity of antigen presenting cells (APC), such as DC and macrophages, together with the cytokines produced in the inflamed area, stimulate the adaptive response with the involvement of T helper cells. It is known that the predominant T cell type in Hp-induced inflammation is Th1 [56]; however, it has been demonstrated that also other T cells are involved in the immune response against Hp: the presence in infected mucosa of IL-17 suggests a role for the Th17 subset [57]; moreover, it has been found that Hp stimulates the proliferation of regulatory T cells (Treg) that limit the proliferation of T effector cells

preventing the risk of a destructive inflammation and probably representing one of the mechanisms responsible for the pathogen persistence [58].

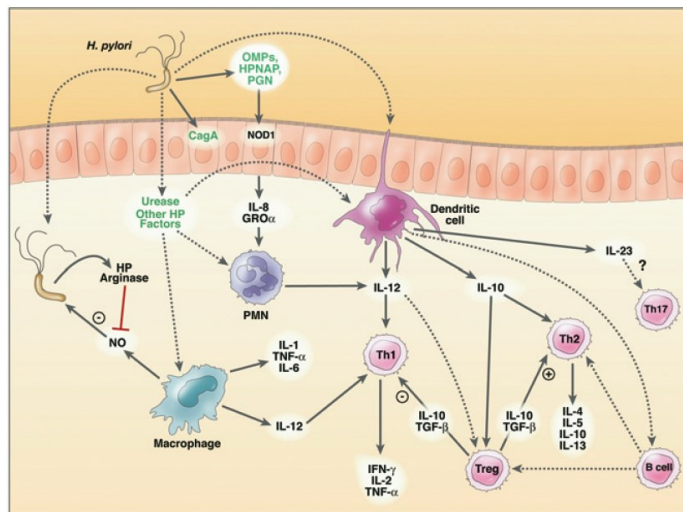


**Figure 6: Schematic overview of the immune response to *Hp*. Dotted lines represent more speculative components of the complex interaction between the bacterium and the host immune system. Image adapted from [59]**

### 2.5.1 Macrophages in *Hp* infection

Although it is clear that the ability of the bacterium to establish a persistent infection relies on the balance between inducing an adaptive immune response and the ability of escaping from it, it is still unclear the role of the innate immunity and what leads to the inability of T lymphocytes to clear the bacterial infection.

It has been demonstrated that during *Hp* infection, phagocytic cells contribute to maintaining high levels of *Hp* loads in the stomach rather than contributing to bacterial clearance [60]. In accordance, computational modelling of immune response against *Hp* predicted that macrophages have a central role in regulating the mucosal immune response [61]. However, the molecular mechanisms through which *Hp* manipulates the macrophage functions are still not fully elucidated.

Up to now there are evidences about the ability of the bacterium to inhibit the killing by nitric oxide (NO).

NO is an antimicrobial agent and its action is based on the covalent binding to DNA, proteins and lipids, thereby leading to the inhibition or killing of the target pathogen.

NO is generated by the inducible enzyme NO synthase (iNOS), which has been shown to be up-regulated by macrophages *in vitro* and *in vivo* upon *Hp* infection. Despite the fact that iNOS production is induced in macrophages, *Hp* still persists, which suggests that the

bacterium has developed mechanisms to avoid NO-dependent killing. Indeed it is reported that Hp possesses an enzyme arginase, which competes with macrophages for the iNOS substrate L-arginine, enhancing the survival of the bacterium, by preventing NO production by host cells. In accordance, arginase-deficient Hp are efficiently killed by macrophage-derived NO, resulting in an attenuated ability of the bacterium to colonize mice *in vivo* [62].

Another potential factor that may contribute to the failed immune response is the ability of the bacterium to avoid effective phagocytosis by macrophages. It has been shown that although Hp can be rapidly internalized into phagosomes, Hp-containing phagosomes undergo extensive clustering and fusion resulting in the formation of structures, named “megosomes”, containing large numbers of live bacteria [63]

Both mechanisms help to elucidate how Hp evades the clearance by the host immune system; still, other types of manipulation could be involved.

### **2.5.2 T lymphocytes in Hp infection**

T helper cells orchestrate host defense against pathogens via different types of effector function.

T helper CD4<sup>+</sup> cells are major effector cells in the immune response to Hp. Historically, they were divided into two main subsets, depending on the different pattern of cytokines released. Th1 cells produce high levels of IFN- $\gamma$  and IL-2 and are responsible for the so-called cell-mediated immune response, whereas Th2 lymphocytes express abundant levels of IL-4 and IL-5 cytokines and induce the activation of B lymphocytes. It has been demonstrated that Hp-related inflammation is characterized by a predominant Th1 polarized response [56]. In response to Hp infection, gastric epithelial cells produce IL-18 and it is known that some bacterial products (such as HP-NAP) stimulate the release of IL-12 and IL-23; all these cytokines drive T cell differentiation toward the Th1 profile [65][42]. Th1 lymphocytes produce huge amounts of IFN- $\gamma$  and TNF- $\alpha$  that are responsible for the severe mucosal damage.

Recently, it has been demonstrated that also IL-17 is increased in Hp-infected patients, suggesting that also the Th17 response is crucial for Hp-induced inflammation [57].

Although an apparently vigorous immune response is mounted, infected patients usually fail to clear the infection, suggesting that the bacterium has evolved strategies in order to overcome and escape the host immune response (Figure 7).

Two virulence factors have been specifically implicated in the manipulation of human T cells. VacA inhibits T cell proliferation by interfering with the T cell receptor-IL-2 signalling pathway preventing the nuclear translocation of the T cell transcription factor NFAT and its subsequent transactivation of T cell-specific immune response genes. The other virulence factor involved in the impairment of T cell response is the  $\gamma$ -glutamyl-transpeptidase (GGT), a secreted protein that inhibits T cell proliferation by inducing G1 cell cycle arrest through disruption of the Ras signalling pathway [66].

Moreover, it has been shown that Hp activates Treg proliferation both in mice and in humans, and while limiting the extent of the immunopathology, they contribute to an increase in bacterial colonization [67]; indeed, it has been demonstrated *in vivo* that the depletion of Treg cells facilitate the clearance of Hp in infected animals [68].

Treg are able to suppress T cell responses, either via cell-to-cell contact or by soluble factors, such as IL-10 and TGF- $\beta$ . They are also able to suppress antigen specific lymphocytes and an abnormal Treg activation by microbial antigens may represent a mechanism of Hp evasion from the host defence.

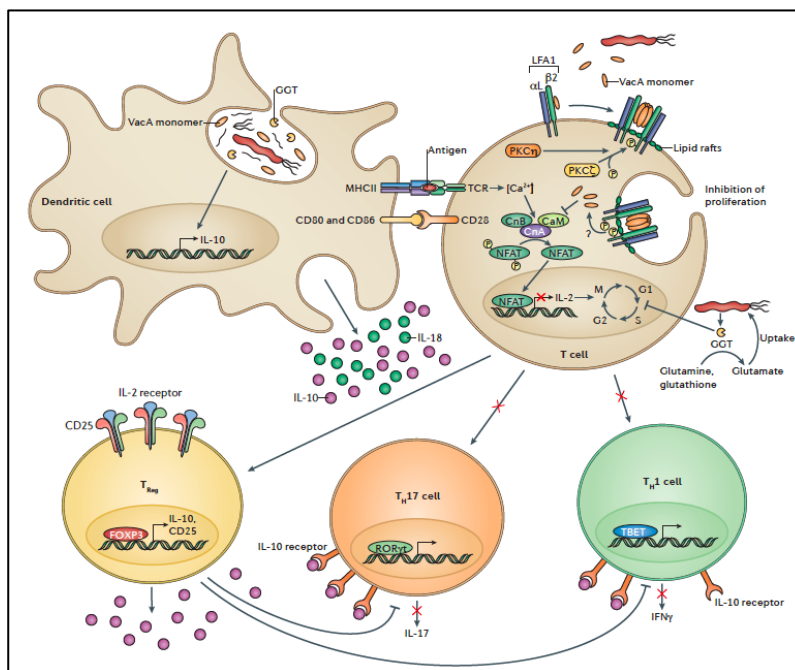


**Figure 7: Hp impairs T cell-mediated immunity blocking Th1 and Th17 proliferation, and promoting Treg proliferation. Image adapted from [66]**

## 2.6 Hp and miRNAs

Only a small percentage (around 2%) of all transcripts (RNAs) are effectively translated into proteins. There are increasing evidence about the biological importance of non-coding transcripts and in particular, among them, micro RNAs (miRNAs) have been proved to function in RNA silencing and post-transcriptional regulation of gene expression.

miRNAs are 20 to 24-nucleotides long RNAs and their deregulation have been linked to many pathological conditions. Most of the miRNA genes are located in intronic regions and are transcribed by RNA polymerase III. The primary transcripts contain typical hairpins structure that are recognized and cleaved by the complex DGCR8, which contains the ribonuclease Drosha. The product of this cleavage is a pre-miRNA that is recognized by Exportin-5 (Exp-5); Exp-5 is responsible for the transport from the nucleus to the cytoplasm.

Once in the cytoplasm, the pre-miRNA is transferred to the RISC loading complex (RLC) where the ribonuclease Dicer, in cooperation with other proteins of the complex belonging to the argonaute (AGO) family, cleaves the pre-miRNA to generate a miRNA-miRNA duplex. Only one miRNA strand represents the mature form and it is loaded onto AGO to form the biologically active complex miRISC; the other strand is sent to degradation.

The miRISC recognizes and binds a short sequence of 2 to 6 nucleotides located on the 3' untranslated region (UTR) of mRNAs, thus resulting in the reduced translation and stability of the target mRNA (Figure 8) [69]. Since the target sequence is very short, a single miRNA is able to modulate the expression of a great number of genes, being implicated in the control of several biological processes.

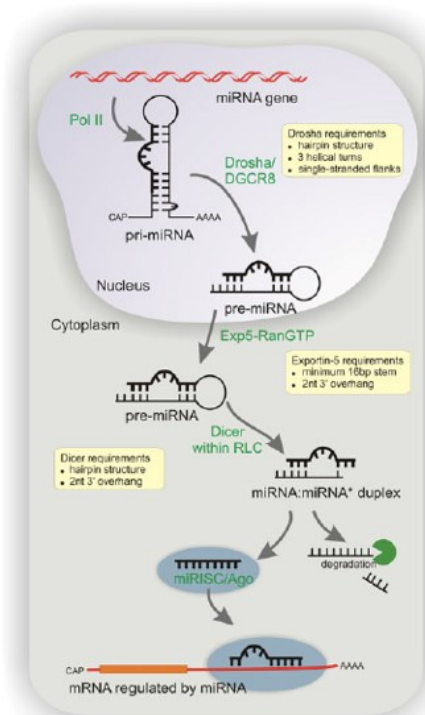


**Figure 8: miRNA biogenesis and activity.** Sequential processing reactions of the primary transcript by Drosha in the nucleus and of pre-miRNA by Dicer in the cytoplasm are presented schematically (details are given in the text). The structural requirements for Drosha, Exportin-5 and Dicer are highlighted in the yellow boxes. Image adapted from [69]

It is already known that Hp infection impacts on miRNA expression. Studies *in vitro* on DC infected with Hp revealed the up-regulation of miR-146 and miR-155.

MiR-146 targets and silences the mRNA encoding TNF-receptor associated factor and that encoding IL1 $\beta$  receptor-associated kinase, which are key adapter in the TLR/NF- $\kappa$ B pathway. MiR-155 is implicated in the regulation of many genes involved in the NF- $\kappa$ B pathway such as Fas-associated protein with death domain (FADD), I $\kappa$ B kinase (IKK) and NF- $\kappa$ B inducing kinase (NIK) [70].

Due to the association with NF- $\kappa$ B activation, a pathway strongly activated during Hp infection and Hp-driven MALT lymphoma, these miRNAs are of special interest in Hp-mediated immune pathologies.

Another miRNA, named miR-210, was found down-regulated in Hp-infected gastric epithelium and the modulation of its expression is shown to correlate with the increased expression of STMN1 (stathmin1, also termed oncoprotein 18 or metablastin) and DIMT1 (demethyladenosine transferase 1). STMN1 is a well-known protein upregulated in solid tumors and is involved in the initiation of tumor development, whereas biological functions of DIMT1 are still unknown in cancer. However, the overexpression of these two genes in tumor gastric cancer cell lines *in vitro* is reported to lead to increased cell proliferation, suggesting that it could have a role in the induction of chronic gastric disease, including cancer, during Hp infection [71].

In gastric epithelial cells miRNAs are involved in the epithelial-mesenchymal transition (EMT). EMT is a process by which epithelial cells lose their cell polarity and cell adhesion, and gain migratory and invasive properties to become mesenchymal stem cells, being implicated in the initiation of metastasis for cancer progression. MiR-200a, -200b, -429 cluster expression is modulated by Hp and this modulation is supposed to support metastasis, by regulating the expression of the EMT-activator zinc finger E-binding homebox 1 (ZEB1). ZEB1 is overexpressed in Hp infected cells, it is found in great amount in gastric biopsies from Hp-positive patients and it is known to promote tumor cell dissemination [72][73].

## **3 Materials and methods**

### **3.1 Monocytes isolation from buffy coat**

Human monocytes were obtained from buffy coat, derived from healthy donors, from the blood transfusion centre of the University Hospital of Padova.

Blood was diluted 1:4 with sterile PBS without  $\text{Ca}^{2+}$  and  $\text{Mg}^{2+}$ ; 5% dextran was added diluted 1:5 and erythrocytes left to settle for 30 min. Supernatant containing white blood cells was collected and centrifuged 10 min at 600 rpm. Cell pellet was resuspended in 15 ml of sterile PBS, stratified on Ficoll-Paque and centrifuged 20 min at 1500 rpm without brake and accelerator. Lympho-monocytes were collected, centrifuged 5 min at 1300 rpm, and then stratified on Percoll (GE-Healthcare) gradient (15.71 ml RPMI 1640, 10% FCS (v/v), HEPES 4 mM (Invitrogen), 50  $\mu\text{g}/\text{ml}$  gentamycin, 285 mOsm + 15.54 ml 10% Percoll in 10x sterile PBS 285 mOsm), and centrifuged 20 min at 1500 rpm without brake and accelerator. Monocytes were recovered and centrifuged 5 min at 1300 rpm, then the cells were resuspended in RPMI 1640, 2% FBS, 50  $\mu\text{g}/\text{ml}$  gentamycin.

#### **3.1.1 Differentiation of monocytes into macrophages**

Monocytes, diluted to the final density of  $5 \times 10^5$  cells/ml, were seeded in 24 well plates (1 ml per well), in order to separate them from contaminating lymphocytes by adherence. After 1 h of at  $37^\circ\text{C}$  5%  $\text{CO}_2$ , cells were washed twice using RPMI 1640, 2% FBS, 4 mM HEPES, 50  $\mu\text{g}/\text{ml}$  gentamycin, and once with RPMI 1640, 20% FBS, 4mM HEPES 50  $\mu\text{g}/\text{ml}$  gentamycin; this step is required for removing non-adherent cell (i.e. dead cells, lymphocytes, erythrocytes). After washing, cells were incubated in 500  $\mu\text{l}/\text{well}$  RPMI 1640, 20% FBS, 4 mM HEPES 50  $\mu\text{g}/\text{ml}$  gentamycin containing 100 ng/ml M-CSF (ORF Genetics) for three days. At the third day, 200  $\mu\text{l}$  of medium were replaced with 300  $\mu\text{l}$  of RPMI 1640, 20% FBS, 4 mM HEPES 50  $\mu\text{g}/\text{ml}$  gentamycin, containing 100 ng/ml MCSF. After further three days macrophages are completely differentiated and can be treated for different time points with the appropriate stimuli.

### **3.2 Hp growth**

Hp can be easily cultured on blood agar plates at  $37^\circ\text{C}$  under microaerophilic condition. After 2 or 3 days of incubation colonies appear small and translucent.

When cultured under favourable conditions, bacteria have the characteristic spiral shape with flagella originating from one pole; on the contrary, aging or exposure to various unfavourable conditions (such as nutrient deprivation, pH adjustment and even antibiotics), cause the conversion to the coccoid form. It is not clear what is the precise function of this form and if it has a role in the pathogenesis, thus, for our experiments, we used only bacteria that appeared in the classical spiral and motile form when observed at the optical microscope.

### 3.2.1 Growth on plate

Plate for *Hp* culturing were constituted as it follows: Columbia Blood Agar Base (Oxoid) supplemented with: 5µg/ml Vancomycin (Sigma), 2.5µg/ml Trimethoprim (Sigma), 2.5 µg/ml Cefsulodin (Sigma), 2.5 µg/ml Amphotericin B (Sigma), 0.2% β-cyclodextrin (Sigma), 5% defibrinated horse blood (Oxoid).

For solid plate, 19 g of Columbia agar were added to 500 ml of milli-Q water. The solution was boiled to dissolve the powder and sterilized by autoclaving. The solution must be cooled to 56°C in a water bath for 30 min. Antibiotic were aseptically added, together with β-cyclodextrin to 0.2% final concentration and 25 ml of horse blood (5% final concentration). 25 ml were added in each sterile Petri dish (10 cm diameter). Plates were cooled at room temperature and then stored at 4°C.



**Figure 9: Hp growth on agar plate.**

### 3.2.2 Hp infection experiments

Colonies were taken directly from plates and suspended in RPMI 20% FBS 4 mM HEPES without any antibiotic. Bacterial count was performed by determining the optical density



(OD) at 600 nm (1 OD =  $10^9$  Colony Forming Units (CFU)/ml). The bacterial density adopted for infecting the cells was  $5 \times 10^5$  CFU/ml.

Before proceeding with the infection experiments, bacteria motility was verified at the optical microscope.

### **3.3 Flow cytometry**

Flow cytometry is a laser-based technology used for analysing the expression of antigens, both intracellular or exposed on the cell surface, taking advantage of fluorochromes-labeled antibodies specific for the antigen of interest. Briefly, when a cell suspension is run through the cytometer, sheath fluid is used to hydrodynamically focus the cell suspension through a small nozzle. The tiny stream of fluid takes the cells past the laser light one cell at a time.

Light scattered from the cells or particles is detected as they go through the laser beam. A detector in front of the light beam measures forward scatter and several detectors to the side measure side scatter. Fluorescence detectors measure the fluorescence emitted from positively stained cells or particles.

Fluorochromes used for the detection of target proteins emit light when excited by a laser with the corresponding excitation wavelength. These fluorescent stained cells or particles can be detected individually.

Forward and side scattered light and fluorescence from stained cells are split into defined wavelengths and channelled by a set of filters and mirrors within the flow cytometer. The fluorescent light is filtered so that each sensor will detect fluorescence only at a specified wavelength. These sensors are called photomultiplier tubes (PMTs)

As the fluorescing cell passes through the laser beam, it creates a peak or pulse of photon emission over time. These are detected by the PMT and converted to a voltage pulse, known as an event. The total pulse height and area is measured by the flow cytometer. The measured voltage pulse area will correlate directly to the intensity of fluorescence for that event.

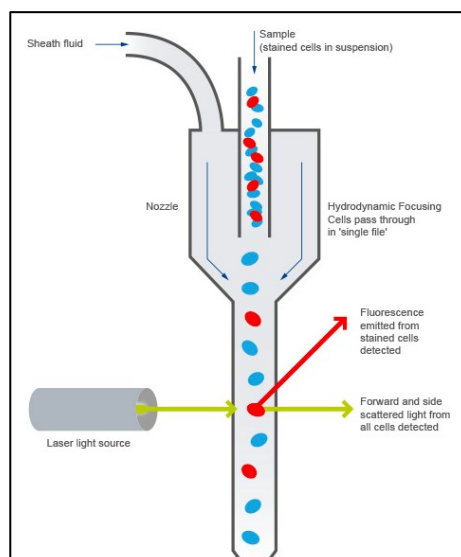


**Figure 10:** Schematic representation of a flow cytometer; sheath fluid focuses the cell suspension, causing cells to pass through a laser beam one cell at a time. Forward and side scattered light is detected, as well as fluorescence emitted from stained cells. Image adapted from [www.abcam.com](http://www.abcam.com)

For the experiments, cells were harvested from culture plates using 5 mM Na-EDTA in PBS pH 7.5 and incubated for 15 min at RT with 10% human serum to saturate Fc receptors.  $5 \times 10^5$  cells were stained with a monoclonal antibody anti-CD300E (clone UP-H2, Abcam), followed by a goat anti-mouse Alexa Fluor 488 antibody (ThermoFisher). The cell viability dye eFluor780 (ThermoFisher) was used to exclude dead cells from the analysis. Cells were resuspended in FACS buffer (PBS, 1% BSA) and analyzed by a six-color FACSCanto II (Becton Dickinson). Forward and side scatter light were used to identify cell populations. Values were expressed as the ratio of the mean fluorescence intensity (MFI) of CD300E over the MFI of the secondary antibody. All data were analyzed using FlowJo software, version 10.3 (Tree Star Inc.).

For the expression of HLA-DR, macrophages were either infected or not with Hp for 48 h; cells were harvested and plated at a density of  $2.5 \times 10^5$  per well in 24-well plates previously coated with the monoclonal antibody anti-CD300E (clone UP-H2, Abcam) or control IgG (MOPC-21, Abcam). After 24 h, cells were collected and stained with a monoclonal antibody anti-HLA-DR APC (clone L243, BD Bioscience); the cell viability dye eFluor780 was used to exclude dead cells from the analysis. Cells were resuspended in FACS buffer (PBS, 1% BSA) and analyzed by flow cytometry. All data were analyzed using FlowJo software.

### **3.4 Phagocytosis assay**

Phagocytosis assay was performed on macrophages, either infected or not with Hp for 48 h, after a 3 h-stimulation with the monoclonal antibody anti-CD300E or with control IgG (as detailed above). Cells were collected, counted and diluted at  $2 \times 10^6$  cells/ml in RPMI 0.2% BSA; after 30 min at 37°C, cells were seeded on pre-chilled 96-well plate ( $10^5$  cells/well in 50  $\mu$ l) and kept at 4°C for 20 min. 50  $\mu$ l of pHrodo™ Green S. aureus BioParticles® Conjugates (ThermoFisher) in RPMI 0.2% BSA (1 mg/ml) were added to the cells. Immediately after the addition of particles (time 0), cells from 3 wells were harvested, collected in FACS tubes and washed once in cold PBS. Plate was transferred at 37°C and, after 15 and 30 min, cells from 3 wells per time point were harvested and processed as above. Phagocytosis was determined by flow cytometry. A gate was selected to identify green fluorescence positive cells (cells that engulfed the particles); MFI was obtained from the selected cell population and data were analyzed by FlowJo software. Phagocytic Index was determined by multiplying the % of fluorescent cells with the MFI value for each sample. Data obtained at 15 and 30 min were normalized on those at time 0 and expressed as arbitrary units (A.U.).

### **3.5 Patients**

The cases considered in this study were retrospectively collected from the Surgical Pathology and Cytopathology Unit at the University of Padova (January 2003 to December 2011). All patients were white and native of the Veneto region, and they underwent endoscopy at Padova University Hospital. The institute's ethical regulations on research conducted on human tissues were followed. The study was conducted on a total of 40 endoscopic biopsy samples obtained from different biopsy sets and all collected from oxyntic proximal mucosa (i.e. gastric corpus). The series included: 1) normal gastric oxyntic mucosa obtained from dyspeptic patients, as control (n = 10); 2) mucosa from Hp – (negative) non-atrophic chronic gastritis (n = 10); 3) mucosa from Hp + (positive) non atrophic chronic gastritis, before Hp eradication therapy (n = 10); and 4) mucosa from the same patients as in 3), who underwent clinical and histological remission, after Hp eradication. Hp was assessed by histology (modified Giemsa staining) and confirmed by clinical history, rapid urease testing, and/or ELISA (Hp-specific IgG Abs; GastroPanel, Biohit HealthCare). Two trained gastrointestinal pathologists, blinded to any of the patients' endoscopic or clinical information, jointly assessed the original slides (H&E, Alcian blue–periodic acid schiff, and Giemsa for Hp).

### **3.6 Immunohistochemistry**

Formalin-fixed paraffin embedded tissue sections were stained with a rabbit anti-CD300E polyclonal antibody (Sigma-Aldrich). On appropriate antigen retrieval (water bath at 98°C for 40 min in ethylenediaminetetraacetic buffer pH 8.0), reactivity was revealed using NovoLink Polymer horseradish peroxidase-linked (Leica Biosystems) followed by Diaminobenzidine (DAB). Characterization of CD300E positive cells was performed by double immunohistochemistry. After completing the first immune reaction, the second was realized using a monoclonal primary antibody to CD163 (clone 10D6, ThermoFisher), visualized using Mach 4-287 AP (Biocare Medical), followed by Ferangi Blue (Biocare Medical) as chromogen. Quantification of CD300E-expressing cells was performed on at least 5 high power fields (HPF) on sections double stained for CD300E and CD163. Immunostained sections were photographed using the DP-70 Olympus digital camera mounted on the Olympus BX60 microscope, and the digital pictures (each corresponding to 0.036 mm<sup>2</sup>) were used for cell count. Values were expressed as the mean ± SD.

### **3.7 Protein extraction from cells and protein quantification**

For protein extraction 10<sup>6</sup> cells were seeded on a 12-well plate and stimulated with appropriate stimuli in RPMI 1649, 20% FBS, 50 µg/ml gentamicin and 4 mM HEPES at different time points. Cells were collected, washed in ice-cold PBS and lysed with ice-cold Triton X-100 lysis buffer (1% Triton X-100, 150 mM NaCl, 20 mM HEPES (pH 7.5), 50 mM NaF, 1 mM sodium orthovanadate, 1 mM EGTA, 2% PMSF, and 1% protease inhibitors) for 30 min on ice. Lysates were centrifuged at 12,000 x g for 20 min at 4°C, and the supernatants were collected and quantified on 96 well-plate using BCA Assay according to manufacturer's instructions. The plate was placed into a plate reader (Packard Fusion) and the optical density at 562 nm determined for each well.

### **3.8 Western blot**

Equal amounts of proteins were resuspended in NuPAGE LDS sample buffer (Novex, Life Technologies) supplemented with 50 mM of DTT and denatured for 5 min at 100°C. Samples were separated electrophoretically in NuPAGE Bis-Tris 4-12% polyacrylamide gel (Novex, Life Technologies) and proteins were subsequently transferred onto PVDF membranes (Amersham). Membranes were blocked with 5% non-fat milk in Tris buffer saline

(TBS, 50 mM Tris-HCl pH 7.6, 150 mM NaCl) containing 0.1% Tween20<sup>®</sup> (Sigma-Aldrich) and antigens were revealed using a rabbit anti-CD300E polyclonal antibody (1:200, Sigma-Aldrich) and a monoclonal anti-HSP90 antibody (1:10000, Origene). Blots were washed three times with TBS plus 0.1% Tween20<sup>®</sup> and incubated for 1 h at RT with horseradish peroxidase-conjugated anti-rabbit (Millipore) or anti-mouse IgG secondary antibody (Novex, Life Technologies), respectively. Blots were developed with enhanced chemiluminescence substrate (EuroClone) and the protein bands were detected using ImageQuant<sup>™</sup> LAS 4000 (GE Healthcare Life Science).

### **3.9 RNA extraction and gene expression analysis**

#### **3.9.1 mRNA extraction**

Total mRNA extraction from macrophages was performed using TRIzol reagent (Thermo Fisher), a monophasic solution of phenol and guanidine isothiocyanate designed to isolate separate fraction RNA, DNA and proteins from cell samples, according to the manufacturer instructions. Briefly, cells were lysed directly in the culture well by adding 300  $\mu$ l of TRIzol and passing the lysate several times through a pipette. The homogenized samples were incubated for 5 minutes at room temperature to permit the complete dissociation of nucleoprotein complexes. Then, 60  $\mu$ l of chloroform were added, tubes were shaken vigorously for 15 seconds and incubated at room temperature for 2-3 minutes. Samples were centrifuged at 12,000  $\times$  g for 15 minutes at 4°C. Following centrifugation, the mixture separated into a lower red, phenol-chloroform phase, an interphase, and a colorless upper aqueous phase which contained RNA. Aqueous phase was transferred into a new tube and RNA was precipitated by the addition of an isovolume of isopropyl alcohol. Following 10 minutes incubation at room temperature, samples were centrifuged again at 12,000  $\times$  g for 15 minutes at 4°C and supernatant was discarded. RNA precipitate was washed two times with 500  $\mu$ l of 75% ethanol RNase free. The RNA was air dried and dissolved in 10  $\mu$ l RNase-free DEPC diethylpyrocarbonate)-treated water.

An aliquot was diluted in water and the absorbance of the solution was measured spectrophotometrically at 260 and 280 nm to determine the purity and the concentration of isolated RNA. Preparations with the ratio A<sub>260</sub>/A<sub>280</sub> higher than 1.8 were considered for further analysis.

### **3.9.2 miRNA extraction**

The protocol used is the same described above. In order to precipitate short RNA (miRNA, in our case) 1.25 volumes of isopropyl alcohol were added to the aqueous phase after the first centrifuge.

### **3.9.3 cDNA synthesis**

Reverse transcription reactions were performed using 1 µg of total RNA.

Firstly, the RNA was denatured in:

DTT	10 mM
First Strand Buffer	1X
DNTPs	0.5 mM
Random pdNG primer	2 µM

RNA was denatured at 72°C for 5 min and then placed on ice.

Samples were retrotranscribed in cDNA using the following mix:

Superscript II (Invitrogen)	140 U
RNasi out (Invitrogen)	98 U
DEPC water	

The retrotranscription was performed in a final volume of 25 µl using the following conditions:

42°C	50 min
95°C	5 min
4°C	

The cDNA obtained from the retrotranscription was directly used to perform Real-Time PCR.

To assess miR-4270 and miR-4459, the TaqMan Advanced miRNA cDNA synthesis kit (Thermo Fisher Scientific) was used following the manufacturer's instruction, and miR-4454 was used for normalization.

### **3.9.4 Real-time PCR**

Real time PCR, also known as quantitative PCR is a technique that allows to monitor the amplification of a target DNA molecule during the PCR in real time, and not at its end as in conventional PCR.

Real time PCR is based on the detection of the fluorescence produced by a reporter molecule, which increases as the reaction proceeds, as a consequence of the accumulation of the PCR product with each cycle of amplification. The initial amount of template DNA is inversely proportional to a parameter measured for each cycle, the threshold cycle (Ct).

The fluorescent reporter molecules include fluorescent DNA-binding dye (i.e. SYBR Green) and gene-specific probes (i.e. TaqMan probes). SYBR Green binds to ds-DNA and in this form produces a much stronger fluorescent signal than unbound dye. Since the dye detects any double-stranded DNA (specific, but also non-specific DNA) it is important to discriminate only the amplification of the target DNA. In order to do this the so called dissociation curve is used: increasing the temperature, the DNA products melt or dissociate, becoming single stranded and releasing SYBR Green resulting in the decrease of the fluorescent signal. The concept is that if the target is one defined sequence, it should have one specific  $T_m$ , while non-target products will have significantly different  $T_m$  values. The melting profiles are translated into peaks; only one peak should be observed (meaning there is only one PCR product). Multiple peaks usually indicate multiple products that can have many sources such as primer dimers or genomic DNA contamination.

In the case of TaqMan probes, they are oligonucleotides labelled with a reporter dye at the 5' end and a non-fluorescent quencher at the 3' end of the probe. During the PCR, the TaqMan probe anneals specifically to a complementary sequence between the forward and the reverse primer sites. When the probe is intact the proximity of the reporter dye and the quencher dye suppresses the reporter fluorescence. During the polymerization, thanks to its 5'-3' exonuclease activity, the Taq polymerase cleaves probes hybridized to the target sequence causing the separation of the reporter dye from the quencher dye. This separation results in the increased fluorescence by the reporter dye. The increase in fluorescence is observed only if the probe is bound to its complementary target sequence and if the target sequence is amplified during PCR; this fact guarantee that non-specific amplification is not detected.

To compare gene expression between biological samples, the  $2^{-\Delta\Delta Ct}$  method was used: firstly, a  $\Delta Ct$  was calculated as the difference between the Ct values for the gene of interest and the housekeeping gene in each sample; the  $\Delta\Delta Ct$  value is the difference between the  $\Delta Ct$  values of an experimental sample and the control sample. PCR, theoretically, amplifies DNA exponentially, doubling the number of target molecules with each amplification cycle, for this reason the  $2^{-\Delta\Delta Ct}$  value represents the fold-change in gene expression, which is expressed in arbitrary units (A.U.).

For each sample, the following PCR mix was prepared:

cDNA	1 $\mu$ l
Primers (50mM)	0.3 $\mu$ l
SYBR green mix	4 $\mu$ l
DNase free H <sub>2</sub> O	2.7 $\mu$ l

PCR reaction was performed in a 384-well plates using the instrument 7900HT Fast Real-Time PCR System (Applied Bioststem), by applying the following cycling parameters:

Initial denaturation	15 min	95°C	} 50 cycles
Denaturation	15 s	95°C	
Annealing	20 s	60°C	
Extension	10 s	72°C	

The pairs of primers used for Real-Time PCR analysis were the following:

CD300E     5'-GGGAGGTGTTGACCCAAAAT-3'  
               5'-AGGACCACGAGCAGGAAGT-3'

CXCL6     5'-GTCCTTCGGGCTCCTTGT-3'  
               5'-CAGCACAGCAGAGACAGGAC-3'

CCL-2     5'-GTCTCTGCCGCCCTTCTGT-3'  
               5'-TTGCATCTGGCTGAGCGAG-3'

CXCL3     5'-AAATCATCGAAAAGATACTGAACAAG-3'  
               5'-GGTAAGGGCAGGGACCAC-3'

MMP14    5'-GCCTTGGACTGTCAGGAATG-3'  
               5'-AGGGGTCACTGGAATGCTC-3'

CCL-22    5'-CGTGGTGAAACACTTCTACTGG-3'  
               5'-CCTTATCCCTGAAGGTTAGCAA-3'

FOXP4    5'-CCAGGATGTTTCGCCTATTTC-3'  
               5'-TTGTGCAGGCTGAGGTTGT-3'

IL17RA    5'-GACCAGGATGCCCCGTCCCT-3'  
               5'-CCCGCTTCACGATGCCGGTT-3'



C1QL2	5'-CAGGGGACGAAGTGTATGTG-3' 5'-CTTGTTATTATTGCCTCCGTGA-3'
SLA	5'-ATTGCCTGGGATCTTGCCAA-3' 5'-TCCATGTGGCTTCTCTTGGC-3'
TLR1	5'-TTCAGTTTCCCACCCATCGG-3' 5'-TGGAATGGATTGTCCCCTGC-3'
GAPDH	5'-AGCAACAGGGTGGTGGAC-3' 5'-GTGTGGTGGGGGACTGAG-3'

For miRNA, qRT-PCR was performed using TaqMan Fast Advanced Master Mix (Thermo Fisher Scientific) in accordance to manufacturer's instructions.

The TaqMan Advanced miRNA Assays used for the PCR were the following:

hsa-miR-4270	5'-UCAGGGAGUCAGGGGAGGGC-3'
hsa-miR-4459	5'-CCAGGAGGCGGAGGAGGUGGAG-3'
hsa-miR-4454	5'-GGAUCCGAGUCACGGCACCA-3'

### **3.10 ELISA assay**

Culture supernatants of infected or not infected macrophages incubated for 24 h with the monoclonal antibody anti-CD300E (clone UP-H2) or control IgG (MOPC-21) were collected for quantification of cytokine content by ELISA assay: specific kit for IL-6 (Immunotools) and IL-1 $\beta$  (eBioscience) were used following manufacturer's instruction.

## **3.11 Microarray expression profiles**

### **3.11.1 mRNA microarray**

200 ng of total RNA was used for Cy3 labelling according to Low Input Quick Amp Labeling Kit (Agilent Technologies). SurePrint G3 Human Gene exp v3 microarrays (Agilent Technologies) were used to identify the genes modulated upon the activation of CD300E. Labelled RNA was hybridized onto microarray slides using a rotational oven at 65°C for 17 h.

After hybridization, both miRNA and mRNA microarray slides were washed and scanned in an Agilent microarray scanner (model G2565CA). Agilent Feature Extraction software version 10.5.1.1 was used for image analysis. Microarray data expression are available in the U.S. National Center for Biotechnology Information Gene Expression Omnibus (GEO) database under the following accession numbers: GSE98641 for miRNA analysis and GSE98639 for mRNA analysis upon CD300E activation.

### **3.11.2 miRNA microarray**

miRNA microarray experiments were performed using the Agilent Human miRNA Microarray 8 x 60K platform (Agilent Technologies) based on miRbase V.19 where 2,006 human miRNAs are represented. 200 ng of total RNA were labelled using miRNA Complete Labeling and Hyb Kit (Agilent Technologies), according to the manufacturer's protocol. Labelled RNA was hybridized onto microarray slides using a rotational oven at 55°C for 22 h.

## **3.12 Microarray data analysis**

### **3.12.1 mRNA microarray analysis**

A meta-analysis approach was applied to identify functional miRNA targets based on the mouse microarray experiments from Weiss et al., 2013 [74]. Raw microarray gene expression data were recovered from GEO database under the accession number GSE42622. Data obtained from infected and non-infected macrophages were quantile normalized and probe expression values that did not pass filter (positive and significant) were set as NA (not available). Probes with more than 50% of NA were excluded from the analysis; this resulted in 29,338 analyzable probes. The same procedure was followed for the analysis of human microarray expression carried out to identify the genes which were modulated upon CD300E activation. 24,836 probes were used to evaluate the effects of CD300E activation. Significance Analysis of Microarray (SAM) test [75] was used to identify genes differentially expressed in mouse microarray. Mouse differentially expressed genes were converted to orthologous human genes using Biomart [76] and NCBI Homologene. Enrichment analysis of differentially expressed genes was performed according to DAVID web tool [77]. Gene Sets Enrichment Analysis [78][79] was used to identify gene sets modulated by CD300E activation. To identify significant pathways it was considered a family-wise error rate (FWER) lower than 0.05. FWER control exerts a more stringent control over false discovery compared to false discovery rate (FDR) procedures [78].

### **3.12.2 miRNA microarray analysis**

Raw microarray data were first filtered for the number of miRNAs presenting an expression value above background (allowed 50% of undetected values for each miRNA) and then normalized according loess cyclic algorithm [80]. Sample clustering was performed according to miRNA expression of detected miRNAs. Pearson correlation and complete linkage were used for cluster analysis, while differentially expressed miRNAs were identified according to SAM analysis [75], maintaining a median false discovery rate (FDR) as 0%. Both analyses were performed using tMev software [81]. miRNA function was inferred according to TAM tool [82], while miRNA targets were recovered by miRDB database [83]. To identify functional miRNA-targets, predicted miRNA-targets were filtered out according to their inverse respect to miRNAs. Corresponding network was analyzed according to NetworkAnalyzer Cytoscape plug-in [84]. BioGrid database v. 3.4 was used to identify functional relationship between different mRNAs described in the network. Node degree parameter was used to size nodes in the network.

## **3.13 Luciferase assay**

### **3.13.1 Cloning of miRNA target expression vector**

Digestion of DNA with the sequence to insert in the plasmid was performed with the restriction endonucleases XbaI and SacI (Promega).

The restriction reaction contained:

- 1 µg DNA
- 5 µl 10X Multicore buffer (Promega)
- 0,5 µl BSA
- Sterile H<sub>2</sub>O up to a final volume of 50 µl

The reaction mix was incubated for 1 h at 37°C.

DNA ligation was performed by incubating the DNA fragments with the linearized pmirGLO Dual-Luciferase miRNA Target Expression Vector (Promega) in the presence of 1 µl of T4 DNA ligase (3 U/µl), 2X Rapid ligation buffer (60 mM Tris-HCl pH 7.8, 20 mM MgCl<sub>2</sub>, 20 mM DTT, 2 mM ATP and 10% PEG) and sterile water to a final volume of 10 µl.

A vector:insert molar ratio of 1:2 was usually used.

The reaction mix was incubated 5 min at room temperature.

*Escherichia coli* TOP10 chemically competent cells (Thermo Fisher), which have been kept on freezer storage, were thawed on ice and used for transformation. The entire ligation mix (10  $\mu$ l) was added to competent cells and the transformation mix was kept on ice for 30 minutes. The cells were heat-shocked for 45 seconds at 42°C and then incubated for 1 h at 37°C with 500  $\mu$ l of Luria-Bertani (LB) broth (10 g/L Tryptone, 5 g/L yeast extract, 10 g/L NaCl).

Bacteria were then plated on LB agar, which contained the antibiotic ampicillin for the transformants selection.

Colonies containing the correct construct were picked up and put on culture at 37°C overnight at 200 rpm in 5 ml of LB.

Cells were harvested by centrifugation for 5 min at 10000  $\times$  g and the plasmid DNA was isolated using the Wizard® Plus SV Minipreps DNA Purification System (Promega) following the manufacturer's instructions.

Briefly, pellets were resuspended with 250  $\mu$ l of Cell Resuspension Solution (Promega), then 250  $\mu$ l of Cell Lysis Solution (Promega) were added and the suspensions were gently inverted 4 times. After 5 min of incubation, 10  $\mu$ l of Alkaline Protease Solution (Promega) were added for other 5 min before stopping the lysis with 350  $\mu$ l of Neutralization Solution (Promega). The suspensions were gently inverted and centrifuged for 10 min at 13000  $\times$  g. Supernatants were applied in the Wizard® SV Minicolumn (Promega) and centrifuged for 1 min at maximum speed; the columns were washed two times with 750  $\mu$ l of Column Wash Solution (Promega) and centrifuged 1 min at 13000  $\times$  g.

The purified plasmids were eluted with 50  $\mu$ l of sterile water, and the concentration and purity were checked at the spectrophotometer. DNA sequencing was performed by BMR Genomics Center of the University of Padova.

### **3.13.2 Luciferase assay**

Macrophages were transfected with miRNA mimics and 100 pg/ $\mu$ l of pmirGLO Dual-Luciferase miRNA Target Expression Vector (Promega) containing target or control sequences. Assays were performed using the Dual-Luciferase Reporter Assay (Promega) and measuring firefly and renilla luciferase activities in a Turner Designs TD-20/20 Luminometer (DLReady™, Promega). miRNA transfections were replicated independently at least three times.

The 3' UTR sequences used for the assay were the following (miRNA binding sites are

evidenced in bold):

CTRL:

GATGTGGGTTAGCAGAGTGTTGAGGGCTGGAGAGGAATGTGTGTAGAGAGATTA  
ACTGGAACCCAGCAAGAAGTGAAAACATGGAGGGAAGAGTTCAGAACCAAGGA  
CAGAGCCCTCGGGGCACCTGCATTTAAAGACAAAGGGTAGGAGGAAGACATTGA  
TCAAGGTGCTGGAGCAGAATCAAACAGGTGGAAGATGAGATCTAGAGTCGACCT  
GCAGGCATGCAAGCTGATCCGGCTGCTAACAAAGCCCGAAAGGAAGCTGAGTTG  
GCTGCTGCCACCGCTGAGCAATAACTAGCATAACCCCTTGGGGCGGCCGCTTCGA  
GCAGACATGATAAGATAATTGATGAGTTTGGACAAACCACA ACTAGAATGCAG  
TGAAAAAAATGCTTTATTTGTGAAATTTGTGATGCTATTGCTTTATTTGTAACCAT  
TATAAGCTGCAATAACAAGTTAACAACAACAATTGCATTCATTTTATGTTTCAG  
GTTTCAGGGGGAGATGTGGGAGGTTTTTTTAAAGCAAGTAAAACCTCTACAAATGTG  
GTAAAATCGAATTTTAAACAAAATATTAACGCTTACAATTTCTGATGCGGTATTTT  
CTCCTTACGCATCTGT

CD300E\_1

GTCCCCTGCCT**CCCT**GGCCCTCATGCCCACTTCCCAAGGGCAAGAATTCCCTGGAA  
GTTGGCCGGGCACCATAGCGAGTGCCTATAATCCCAGCTCAGGAGGCTGAGGCA  
GGAGGATCGGCTGAACGTAAGAGTTCCAGGCCAGCCTGGGCAACATAGAGAGCC  
CTGTCTCAGAGAGAGAGAGAGAGAGAGAGACAGAGAGAGAGACAGAGAGAG  
AGAGAGCGAGAGAGAGAGAGAGAGAGAGAGAAAAGGACGGAGGAAGGGAGGAAA  
AAAATTTTCTGGAGGAGCCTGGCCCTTCATTCTTCTTGGCACAAATGCTTCTCAGG  
CCAGTTTCCCCCAGGGCAATAACTACCTCCTTCTGACAGACAGGAGT**CTCCCT**G  
GGACACACCCCTCACAGCCCCAGCCTTTAGGT

CD300E\_2

CTCCTCTCGTCTTCTGACGCCCTTGGGT**CTCCCT**GGCTTTAAGGCCCTTCT**CTC**  
**CCT**GTAACCAGGCAGTGTGTGGCTGGGCTCAGAACATCTCTGCCTGGGTGGGCC  
ATGGATGAGCTGCTCCAGGTTAAAGTTCTGGGGTGAGTTGAAACAGTAAAGGGA  
GAAGGAGCTGGTGGGTGCCCC

Src-like adaptor (SLA)

CTTCTCTATCCACATCATGACCAAAGGAACCC**CTCCCT**GGTGTCTGATCAGGGCT  
GTGGCATCACGAAACATTGGATCATGACATGTCGGGCGATGCTTGGAAGAGCCC

AGCATGTATGTATGCACACATTGTGTGTGTGGGAAGGACAAAGCCACTCTCACAA  
GAAAGGGCACCAGGACTGCTCTCCAAGGAACTGGACCTGTCCAGACAGTTACAC  
TCCAAGGTCATTGGAGAGAACTTCTGTATGGGCAAGCCTGAGAGGGAGAGGAAA  
CAAAGCTGTGTCCTGGCAGAAGGTCTGGGTTTGCAGATGGGTGCCCTGAATGGA  
ACTACTTTAACTAATCCATAGGGACTTCTGGTATGCTTTCCTCTCTTTTTAAAGGA  
ACTTCGTGACACTAAACATTAGCCCAAAGGACTTCTTAGCCTTCAATTGGGAGAT  
ACCTTTGGTCTGCTCCTGCACCAAAGCCATATGGGTGGAAGTCAGTTGGCCTCCC  
TGGTTCTGCAGAGGGCCAGAAGAATGAGAGAGAGGAAGACTGCTGGCAGGGAA  
ATCTCTAGAGTCGACCTGCAGGCA

Toll-like receptor 1 (TLR1)

GAGATCGTGGACTATGTGGCCAGCCAGGTTACAACCGCCAAGAAGCTGCGCGGT  
GGTGTGTGTTTCGTGGACGAGGTGCCTAAAGGACTGACCGGCAAGTTGGACGCCC  
GCAAGATCCGCGAGATTCTCATTAAAGGCCAAGAAGGGCGGCAAGATCGCCGTGT  
AATTCTAGTTGTTTAAACGAGCTCATTACACATCAAGTGAAAAATATTCCTCCTG  
TTGATATTGCTGCTTTTGGAAAGTTCCAACAATGACTTTATTTTGCATCAGCATAGA  
TGT

MMP14

CGAGCCCCCTCCCCGCAGCCTCCTTGCTTCTCTGTCCCCTGGCTGGCCTCCTTC  
ACCCTGACCGCCTCCCTCCCTCCTGCCCCGGCATTGCATCTTCCCTAGATAGGTC  
CCCTGAGGGCTGAGTGGGAGGGCGGCCCTTCCAGCCTCTGCCCTCAGGGGAAC  
CCTGTAGCTTTGTGTCTGTCCAGCCCCATCTGAATGTGTTGGGGGCTCTGCACTTG  
AAGG

### 3.14 Functional assay

Macrophages were either infected or not with Hp for 48 h; cells were detached with 5 mM Na- EDTA in PBS pH 7.5, harvested and plated at a density of  $2.5 \times 10^5$  per well in 24-well plates previously coated with the monoclonal antibody anti-CD300E (clone UP-H2, 10 $\mu$ g/ml), for 3, 6 and 24 h. Cells and supernatants were collected and stored for RNA extraction and analysis or for ELISA assays.

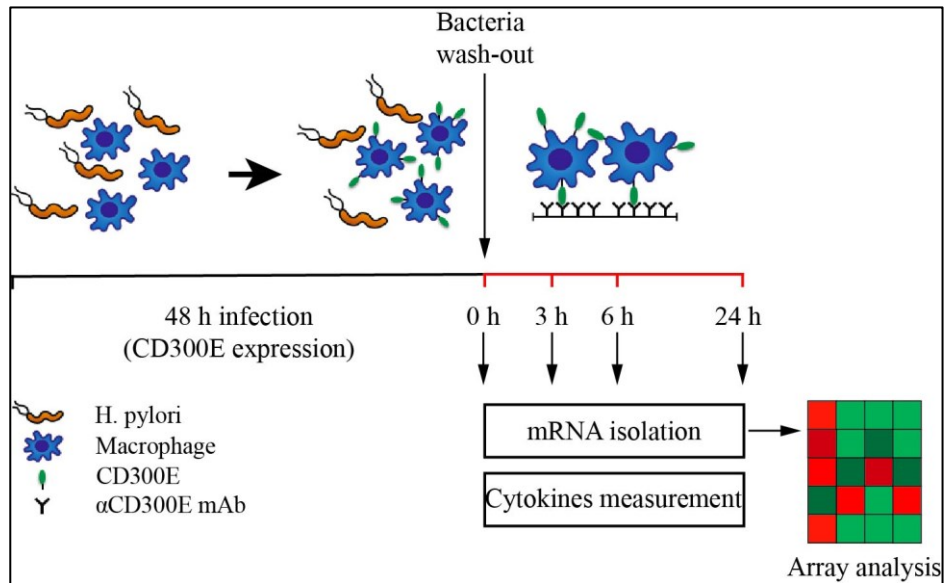


Figure 11: Schematic representation of the protocol used for functional assays.

### 3.15 Proliferation assay

#### 3.15.1 Generation of tetanus toxoid-specific cell clones

Tetanus toxoid (TT)-specific T cell clones were obtained from peripheral blood of three healthy donors, as described [85]. Twenty TT-specific T cell clones were selected for this study.

#### 3.15.2 CFSE-based proliferation assay

$5 \times 10^4$  infected or non-infected macrophages were seeded in 96-well plates pre-coated with  $10 \mu\text{g/ml}$  of the monoclonal antibody anti-CD300E or control IgG for 24 h. After this time, CFSE-stained T cell clones, in medium plus  $0.5 \mu\text{g/ml}$  TT, were added into each well.

Briefly, each clone was harvested and washed two times with RPMI 10% FBS and once with PBS.  $1 \mu\text{l}$  CFSE  $5 \mu\text{M}/10^6$  cell/ml PBS (Celltrace CFSE cell proliferation kit, ThermoFisher Scientific) was added to each cell suspension; after a 20 min staining in the dark, at RT, cells were washed with RPMI 5% human serum, to inactivate CFSE, counted and seeded at the density of  $10^5$  cells/well. The percentage of proliferating T cell clones in response to TT was determined by measuring the CFSE fluorescence by flow cytometry after 18 h of macrophages-lymphocytes co-culture; 5000 events were acquired for each sample.

### **3.16 Statistical analysis**

Data were reported as mean values  $\pm$  SD. Statistical significance was calculated by unpaired Student's t-test. Mann Whitney U test was used for statistical analysis of the differences between experimental groups. p values less than or equal to 0.05 were considered significant. A probability (p) of less than 0.05 was considered significant and was indicated with \*, a p < 0.01 was indicated with \*\* and a p < 0.001 was indicated with \*\*\*.



## 4 Results and discussion

### 4.1 Hp infection modulates miRNA expression in macrophages

With the aim of evaluating miRNA profile induced by Hp infection in macrophages, we adopted human monocyte-derived macrophages as cell model, and we exposed them to live bacteria. We found that, regardless of the infection, 270 of 2,600 detectable miRNAs were expressed in at least 50% of analyzed samples, and the most represented miRNA families were let-7, miR-17, miR-30, and miR-320. Sample cluster analysis, based on the expression of detected miRNAs, revealed a differential expression of miRNAs in cells infected with Hp with respect to control cells (Figure 12), suggesting that Hp infection actually modulates miRNA expression in macrophages. Fifty-five miRNAs were down-regulated and 46 were up-regulated after 24 h infection with Hp. Similarly, 53 miRNAs were down-regulated and 41 were up-regulated in macrophages exposed for 72 h to the bacterium. 26 miRNAs were up-regulated and 23 were down-regulated both at 24 and 72 h (Figure 12). Since Hp infection triggers a chronic inflammation, we reasoned that down-regulated miRNAs, being permissive on the expression of their target genes, were the most interesting to investigate.

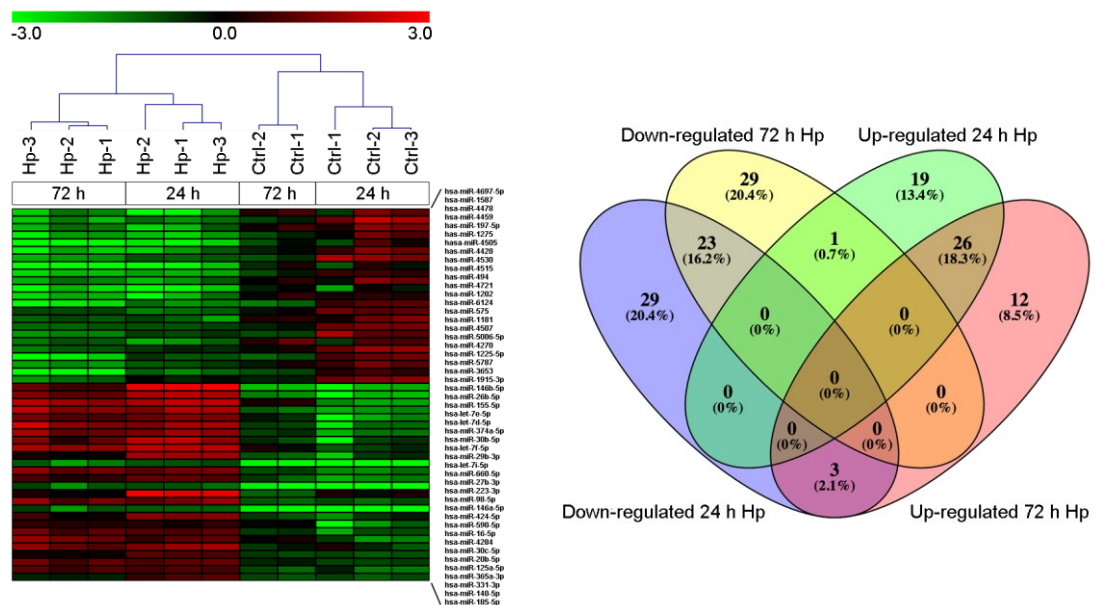


**Figure 12:** miRNA expression in macrophages infected with Hp. Unsupervised cluster analysis of detected miRNAs from Hp-infected macrophages. Heat map represents the expression of differentially expressed miRNAs identified at 24 and 72 h of infection. Gene expression values are relative to the average expression of data collected at T<sub>0</sub> and log scaled. Venn diagram representing distribution of differentially expressed miRNAs.

## 4.2 Identification of miRNA targets

Taking advantage from an already published work on mouse [74], we detected differentially expressed mRNAs in mouse macrophages infected with Hp and identified human orthologous presenting miRNA seed sequences in their 3'-UTR. 1,120 up-regulated and 898 down-regulated probes identified the coding genes activated and inhibited (843 and 763 genes, respectively) by the infection of mouse macrophages with Hp. 646 of 843 and 558 of 763 genes had human orthologous. Down-regulated genes were mainly involved in the production of energy based on lipid oxidation, DNA replication, transcription, and repair, whereas a large proportion of up-regulated genes were related to the immune response. The expression of several mRNAs, up-regulated in mice macrophages infected with Hp, was validated in human macrophages infected with the bacterium (Figure 13). Among them, the most up-regulated at 24 h post-infection were CD300E, CXCL6, CCL2, CXCL3, and matrix metalloproteinase 14 (MMP14), and some of which remained up-regulated longer (72 h post-infection). We reasoned on the possibility that the up-regulated genes were target of Hp-modulated miRNAs. Integrating the expression of miRNA predicted targets and down-regulated miRNAs by Hp infection, we evidenced that 16 of the 23 miRNAs down-regulated both at 24 and 72 h post-infection, actually found a correspondence in the upregulation of predicted targets (Figure 14). Six of 16 (miR- 4530, -4428, -6124, -4459, -1915-3p, and -4270) occupied a central position in the regulation of inflammatory processes (Figure 14).

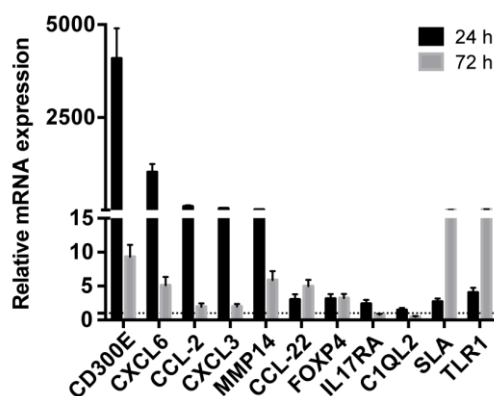


**Figure 13: validation of the expression of immunity-related genes in Hp-infected macrophages.** The expression of some up-regulated genes in mouse macrophages infected with Hp was confirmed in human macrophages after the exposure to live bacteria for 24 and 72 h. All genes considered were up-regulated either at 24 or 72 h of infection. The expression is relative to non-infected macrophages, and dashed line represents not differential expression.

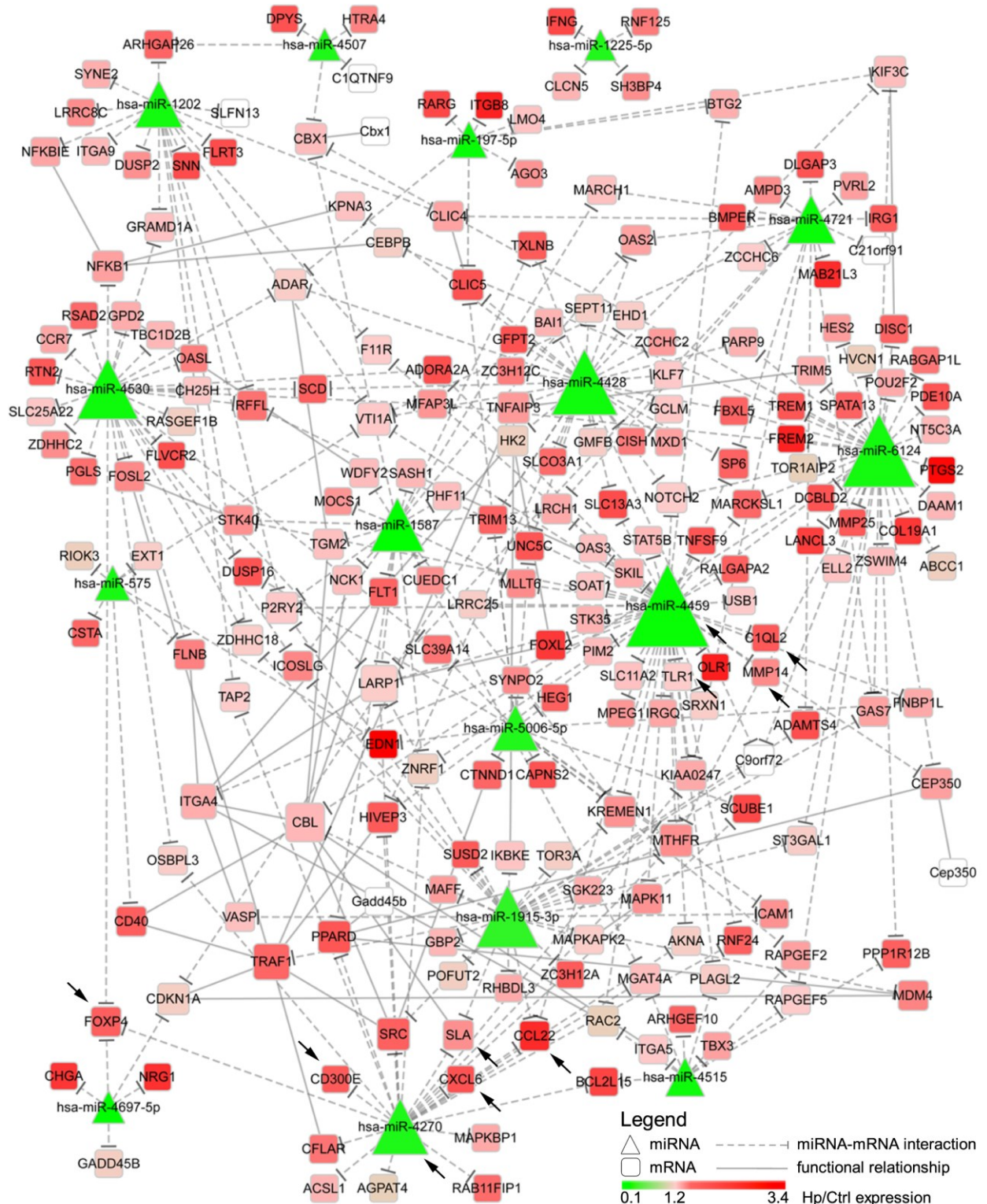


**Figure 14: Integration of microRNAs (miRNAs) and mRNA targets.** The network describes the interactions between miRNAs down-regulated both after 24 and 72 h of Hp infection and the predicted targets. The higher the node size is, the higher the number of edges connected with it is. Color scale mirrors the expression of miRNAs and genes in Hp-infected vs non-infected macrophages (Ctrl). Triangles represent miRNAs, whereas round squares refer to mRNAs. Dashed edges interconnect miRNAs with their targets, whereas filled edges describe functional relationships between different mRNAs. Arrows indicate genes, and miRNAs for whom the expression was confirmed in human derived macrophages by qRT-PCR.

### 4.3 miR-4270 regulates the expression of *CD300E*

We focused our attention on miR-4459 and miR-4270: the first because of the multiplicity of its targets and the second because predicted to target the most up-regulated gene in macrophages infected with Hp, *CD300E*. For both miRNAs, we confirmed by qRT-PCR a down-regulation of about 80% after 24 h and of about 50% after 72 h of infection (Figure 15) and the activation of some of their targets (Figures 13 and 14), with respect to control cells.

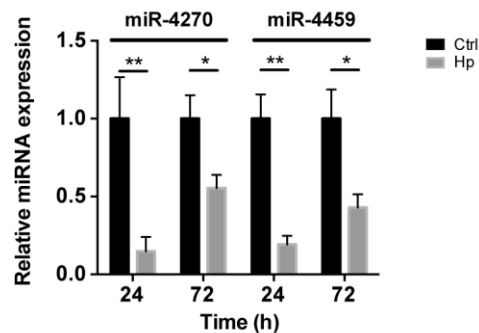


**Figure 15:** qRT-PCR analysis of miR-4270 and miR-4459 in Hp-infected macrophages- target interaction. miR-4270 and miR-4459 downregulation in Hp-infected human macrophages as assessed by qRT-PCR. miRNA expression was evaluated after 24 and 72 h of Hp infection. \* $p < 0.05$ ; \*\* $p < 0.01$

The interaction between miR-4459 and miR-4270 and two of their mRNA predicted targets were also confirmed by luciferase assay. In particular, miR-4459 was confirmed to directly interact with mRNA coding for toll-like receptor 1 (TLR1) and metalloproteinase 14 (MMP14), whereas miR- 4270 was confirmed interacting with mRNA coding for Src-like adaptor (SLA) and *CD300E* (Figure 16).

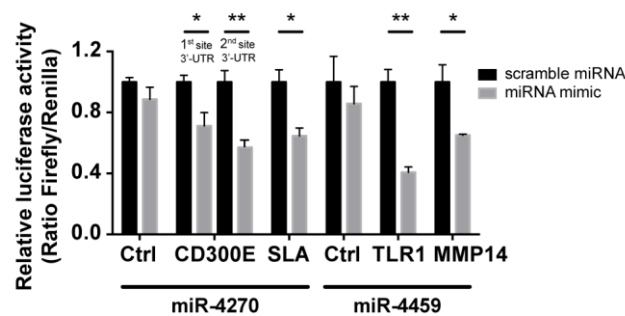


**Figure 16:** validation of miRNAs. Luciferase assay supports the interaction between miR-4459 and TLR1 and matrix MMP14 3'-UTR, whereas miR-4270 was confirmed to interact with SLA and with two sites in the *CD300E* 3'-UTR. miRNA scrambled sequence and 3'-UTR control sequence (Ctrl) did not alter fluorescence for all the interactions tested.

## 4.4 Hp-infected macrophages expose CD300E on the plasma membrane

The CD300 or immune receptor expressed by myeloid cells (IREM) family consists of at least seven surface molecules that are encoded by genes located on chromosome 17 [86].

CD300E was firstly described as a glycoprotein with a single extracellular Ig-like domain expressed by mature monocytes and peripheral blood myeloid dendritic cells; it has got a short cytosolic domain and a positively charged transmembrane sequence which allows the interaction with adaptors such as DAP-12 [87].

Functional experiments performed on monocytes taking advantage from a monoclonal antibody specific for CD300E, that interact with the protein acting as an agonist, have demonstrated that its activation results in the expression of co-stimulatory molecules (CD83, CD86) and secretion of pro-inflammatory cytokines [88]. Thus, CD300E is classified among the activating receptors of the CD300 family.

### 4.4.1 Hp infected macrophages express CD300E

It is reported that the differentiation of monocytes into macrophages leads to the down-regulation of the expression of the immune receptor; thinking about this evidence, we were impressed by the finding that the infection with Hp seemed to revert the expression of CD300E.

As expected, from the comparison between infected and non infected macrophages, we found that the expression of the protein was strongly promoted in the presence of the bacterium, thus resulting in an increase of the basal expression of CD300E (Figure 17)

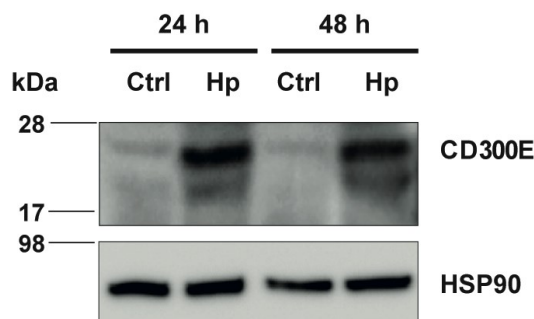


**Figure 17: Western blot of macrophages, before and after infection, developed with a polyclonal antibody anti-CD300E. Although a basal expression of CD300E is appreciable in not infected cells (Ctrl), it is highly induced upon Hp infection. The band between 17 and 28 kDa is consistent with the expected molecular weight of CD300E.**



We also evaluated CD300E expression on the surface of macrophages, monitoring its accumulation through flow-citometry for a period of 72 h and we evidenced that macrophages exposed to Hp had a time-dependent over expression of the protein on the plasma membrane that, after 72 h of infection, was about 10 times over the level of control cells ( $927 \pm 90.51$  vs  $89.5 \pm 14.85$ ; Figure 18)

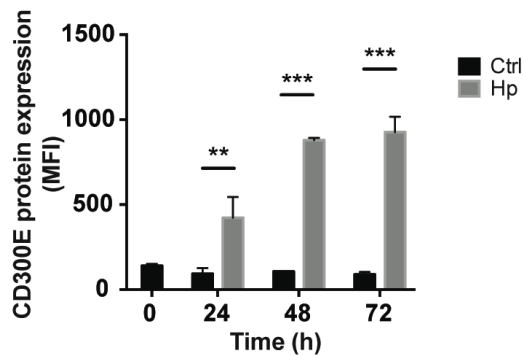


**Figure 18:** Time-dependent expression of CD300E in macrophages infected with Hp, evaluated by cytofluorimeter.

As further proof of the direct interaction of miR-4270 with CD300E mRNA we transfected macrophages with a miR-4270 mimic leading to a significant impairment of the exposition on the plasma membrane of the immune receptor induced by the bacterium (Figure 19); on the contrary, transfection with a scramble miRNA did not affect CD300E expression, which remained at a level comparable to that of infected cells.

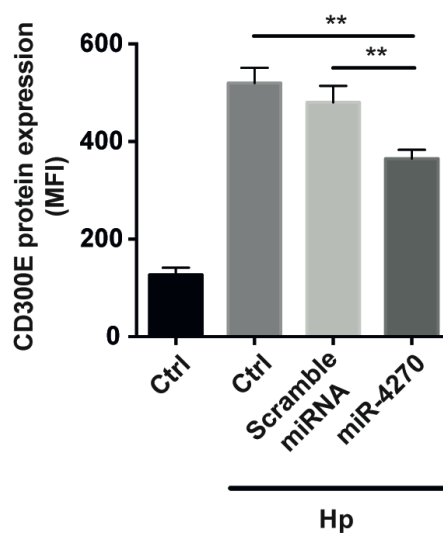


**Figure 19:** Downregulation of CD300E expression in Hp-infected macrophages transfected with miR-4270 mimic. No effect was observed in macrophages upon transfection with a microRNA (miRNA) scramble. Transfection was performed 3 h after starting the infection, and cells were stained for CD300E after 24 h. Control (Ctrl) refers to cells transfected with control sequence

#### 4.4.2 Macrophages infected with *Escherichia coli* don't express CD300E

To verify if CD300E expression by macrophages was strictly dependent on the Hp infection or it was induced also by other bacteria, we evaluated by flow-cytometry the expression of the receptor in macrophages infected with a non pathogenic strain of *Escherichia coli* (Ec).

It was worth noting that, after 24 h of incubation, only in Hp-infected macrophages we observed a significant accumulation of CD300E on the cell membrane, whereas Ec-infected macrophages exhibited the same protein expression than in control cells (Figure 20).

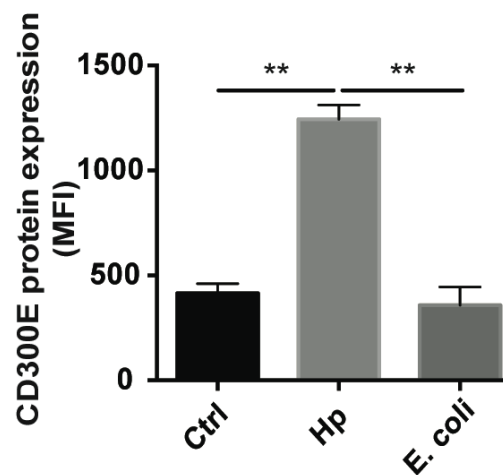
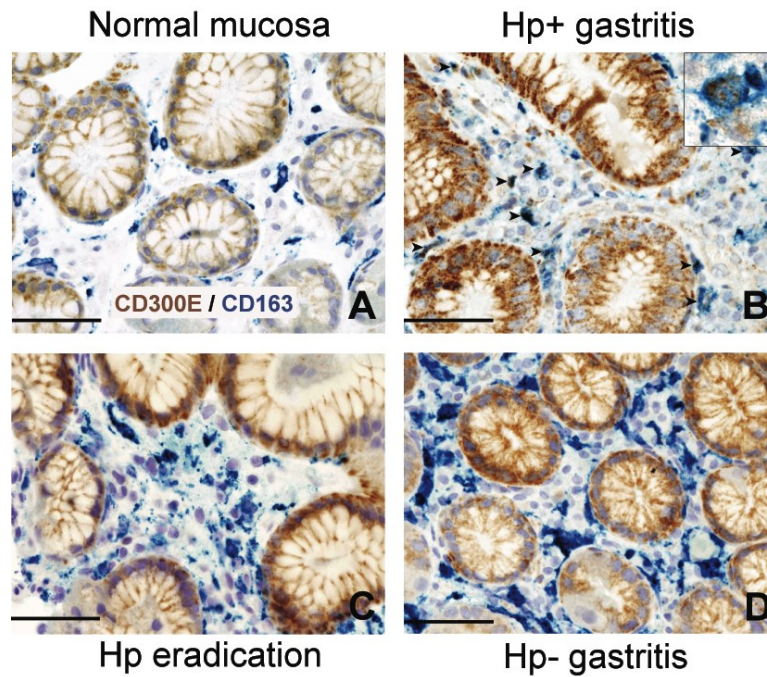


Figure 20: Expression of CD300E in macrophages infected with Hp or with *E. coli*.

#### 4.5 Macrophages expressing CD300E infiltrate the mucosa of Hp-induced gastritis

The evidence that Hp promoted the expression of CD300E in macrophages prompted us to search for an *in vivo* correlation between Hp infection and the presence of macrophages expressing CD300E. We assessed the expression of the receptor on macrophages infiltrating the mucosa of human patients suffering from Hp gastritis. With respect to normal mucosa (Figure 21A), Hp-infected mucosa revealed that a significant proportion of macrophages, identified as CD163<sup>+</sup> cells, were positive for CD300E (Figure 21B). The accumulation of CD300E<sup>+</sup> macrophages strictly relies on the presence of the bacterium, since they were virtually absent in patients that underwent Hp eradication (Figure 21C) as well as in patients with Hp<sup>-</sup>(negative) gastritis (Figure 21D).



**Figure 21:** Expression of CD300E in macrophages infiltrating *Helicobacter pylori* (Hp) gastritis. Sections are from gastric biopsies (A–D) showing normal mucosa (A), Hp+ gastritis, respectively, pre- (B) and post-Hp eradication (C), and Hp– gastritis (D). Sections are stained for CD300E (brown) and CD163 (blue). The arrows and inset highlight CD163<sup>+</sup>CD300E<sup>+</sup> double positive macrophages. Original magnification 400x scale bar 50 mm. Inset 600x.

Notably, the fact that less CD163<sup>+</sup>/CD300E<sup>+</sup> cells were present in the latter condition did not reflect a minor infiltration of macrophages with respect to the infectious gastritis, since they were numerically almost identical in the two conditions (Figure 22).

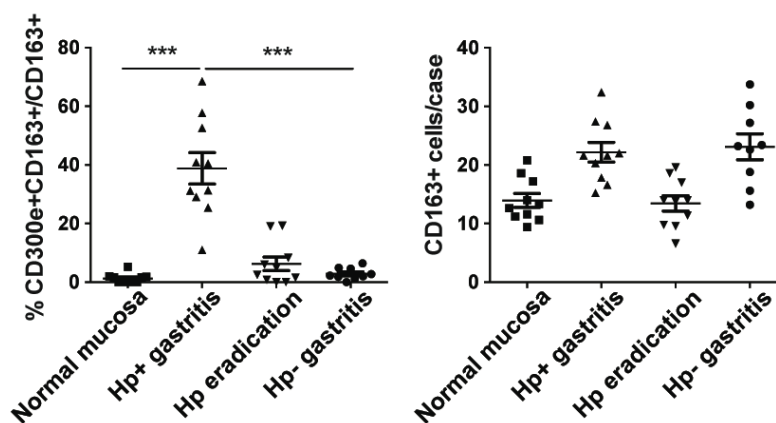


**Figure 22:** Graph showing the percentage of CD300E<sup>+</sup> macrophages (CD163<sup>+</sup>) (\*\*\*)  $p = 0.0002$  vs normal mucosa and \*\*\*  $p < 0.0001$  vs Hp eradication and Hp– gastritis). (F) Graph showing number of CD163<sup>+</sup> macrophages in the cases analyzed.

These results confirmed that the expression of the immune receptor CD300E on macrophages is strictly related to the presence of Hp; moreover, since in the mucosa of Hp- negative



gastritis CD300E is not appreciable, its up-regulation can be considered a hallmark of Hp-infection.

## 4.6 CD300E activation effects on macrophages

To determine the impact of CD300E activation in macrophages infected by Hp, we took advantage of an agonistic soluble anti- CD300E monoclonal antibody (UP-H2), being the natural ligand still unknown [88]. Upon a 48 h infection, macrophages were incubated with the antibody and after a short (3 and 6 h) and a long incubation (24 h), mRNA expression profile was evaluated by micro array technology.

Pathway name	FWER p-value
<b>3 h CD300E activation</b>	
PID_NFAT_TFPATHWAY	0.000
PID_TCR_CALCIIUM_PATHWAY	0.003
PID_CD8_TCR_DOWNSTREAM_PATHWAY	0.011
PID_IL6_7_PATHWAY	0.012
BIOCARTA_INFLAM_PATHWAY	0.016
<b>6 h CD300E activation</b>	
BIOCARTA_INFLAM_PATHWAY	0.000
PID_NFAT_TFPATHWAY	0.002
<b>24 h CD300E activation</b>	
REACTOME_CHEMOKINE_RECEPTORS_BIND_CHEMOKINES	0.003
KEGG_CYTOKINE_CYTOKINE_RECEPTOR_INTERACTION	0.011
PID_TCR_CALCIIUM_PATHWAY	0.025
PID_NFAT_TFPATHWAY	0.031

**Table 1: pathways activated upon CD300E activation. On the left, the pathway name as indicated in the GSEA used databases, and on the right, the family-wise-error-rate (FWER).**

### 4.6.1 CD300E activation establishes a pro-inflammatory profile

In accordance with the definition of activating receptor able to establish a pro-inflammatory profile in monocytes, we observed that a short time activation elicited a pro-inflammatory profile also in macrophages, testified by the activation of pathways related to inflammation, as detailed in Table 1. In order to understand if the modulation of the expression of pro-inflammatory genes was followed by an effective protein overexpression, we measured the amount of IL-1 $\beta$  and IL-6 in the supernatant of activated macrophages by ELISA assay. As shown in Figure 23, 24 h of stimulation with the activating antibody, lead to a significant increase in IL-1 $\beta$  and IL-6 production, with respect to control samples incubated with the isotype control. The effects of CD300E activation were more evident in uninfected cells (Ctrl in Figure 23), probably because the infection with Hp *per se* stimulated IL-1 $\beta$  and IL-6 release by macrophages..

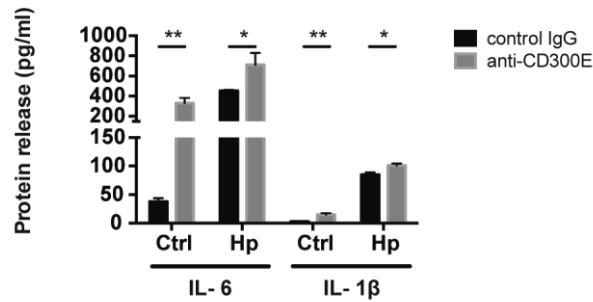


Figure 23: Release of IL-1 $\beta$  and IL-6 by macrophages after the engagement of CD300E.

#### 4.6.2 CD300E activation affects antigen presentation

Interestingly, this activation, which was maintained 24 h after starting the incubation with the anti-CD300E antibody (Table 1), was paralleled by the abatement of the MHC-II-dependent pathway of antigen presentation (Table 2). In particular, we found that mRNAs encoding for HLA-DMA, HLA-DMB, HLA-DOA, HLA-DPA1, HLA-DPB, HLA-DRB1, HLA-DRB3, HLA-DRB4, and HLA-DRB5 were strongly down-regulated (Figure 24).

Pathway name	FWER $p$ -value
<b>24 h CD300E activation</b>	
KEGG_ANTIGEN_PROCESSING_AND_PRESENTATION	0.000
KEGG_LYSOSOME	0.028
REACTOME_MHC_CLASS_II_ANTIGEN_PRESENTATION	0.047

Table 2: Pathways inhibited upon CD300E activation. On the left, the pathway name as indicated in the GSEA used databases, and on the right, the family-wise-error-rate (FWER).

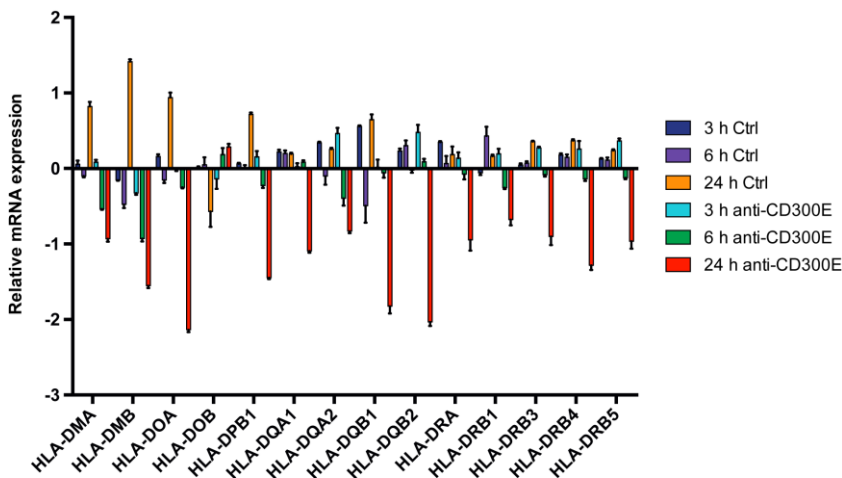
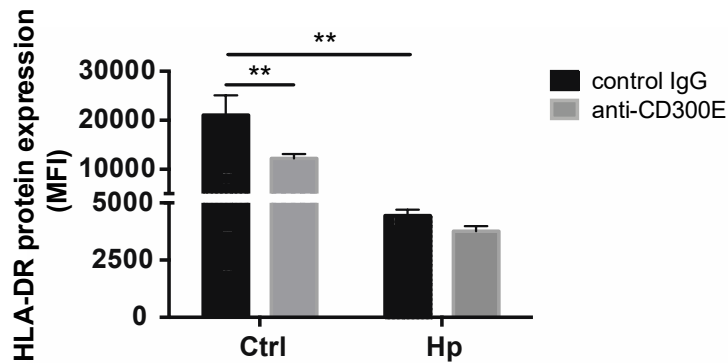


Figure 24: Expression of genes of the MHC-II locus in Hp-infected macrophages upon CD300E activation. Macrophages were infected for 48 h before activating CD300E by cell exposure to the anti-CD300E agonistic monoclonal antibody (clone UP-H2, Abcam) for 3, 6 and 24 h (3 h, 6 h, or 24 h anti-CD300E).

Control cells (Ctrl), infected but not activated by the antibody, were harvested at the same time points. Gene expression is expressed referring to the average expression of the gene in all experiments. Histograms for each gene at each time point represent the average of gene expression of at least three biological replicates. Comparing with the control, genes for MHC-II were down-regulated at 6 and 24 h of CD300E activation.

To validate the impact of CD300E on the modulation of the MHC-II pathway, we determined the expression of HLA-DR on the plasma membrane of macrophages exposed to the agonistic antibody. A 24-h stimulation of CD300E reduced the surface exposure of HLA-DR molecules by ~50% in uninfected macrophages (Figure 25). Surprisingly, the infection of macrophages by Hp led to more than 50% drop of HLA-DR, and this occurred regardless of the antibody stimulation. However, a further decrease by 10% was detected upon anti-CD300E activation (Figure 25).



**Figure 25:** HLA-DR expression in macrophages infected or not with *Helicobacter pylori* (Hp), upon activation of CD300E with the agonistic monoclonal antibody; as control, macrophages were exposed to isotypic IgG (control IgG). Data are shown as mean fluorescence intensity (MFI)  $\pm$  SD of three independent experiments performed with three different cell preparations

Such a decreased expression of HLA-DR functionally affected macrophages resulting in the impairment of the antigen presentation ability to T lymphocytes, as revealed by a proliferation assay (Figure 26). Notably, the activation of CD300E affected the antigen presentation independently from the infection, in accordance to the HLA-DR expression pattern.

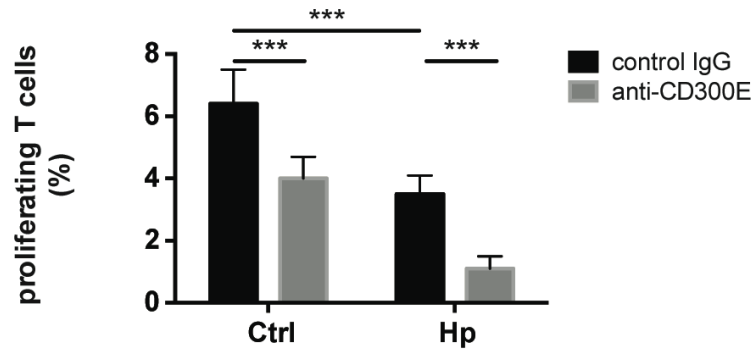
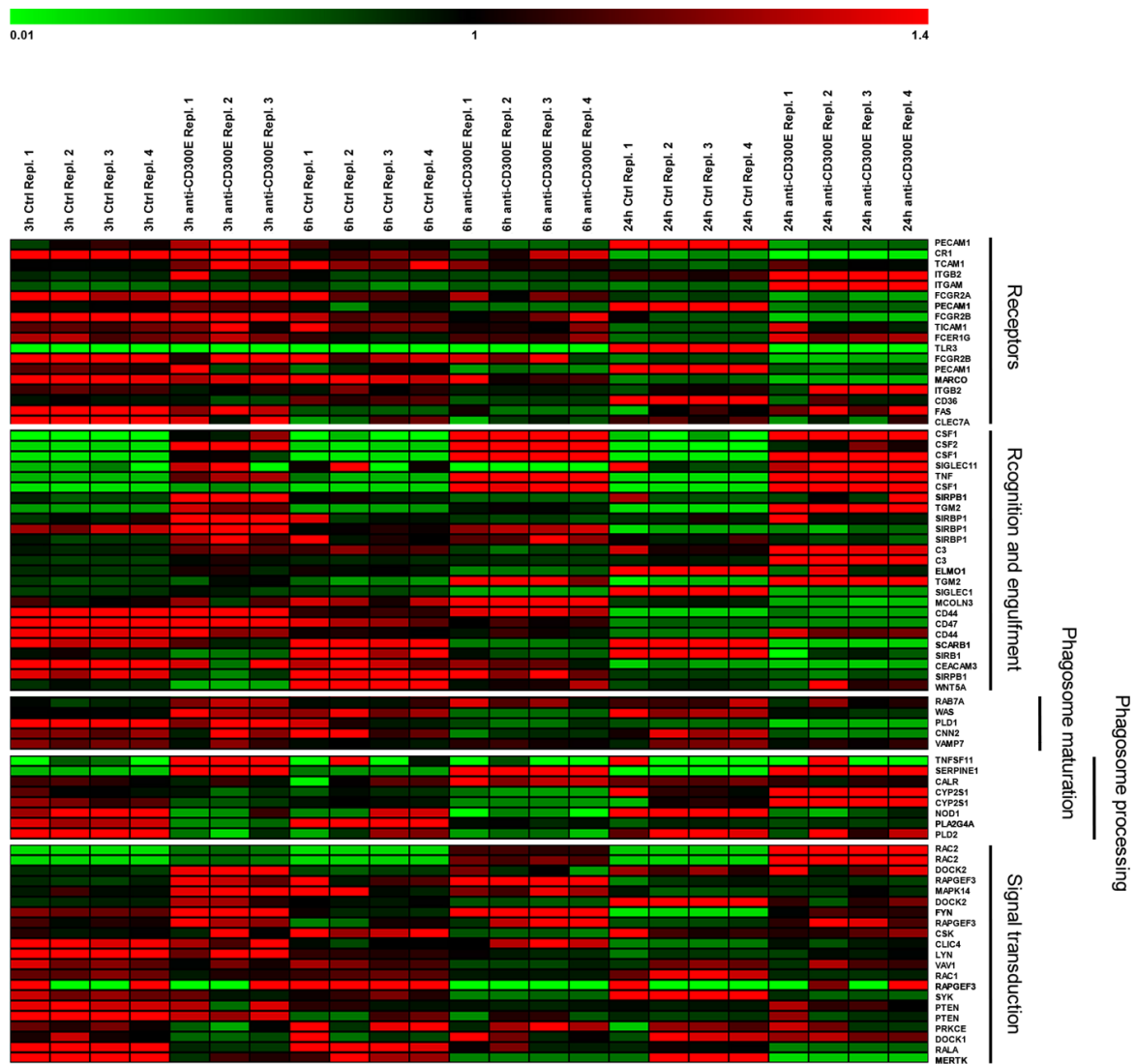


Figure 26: Impact of CD300E activation on the antigen presentation ability of macrophages to T lymphocytes. Data are expressed as percentage of proliferating cells as determined by CFSE-based staining (mean  $\pm$  SD). Two independent experiments were performed with 10 different T cell clones for each experiment.

#### 4.6.3 CD300E activation enhances phagocytosis

Interestingly, despite the pathway of antigen presentation was compromised by the activation of CD300E, phagocytosis was stimulated by the activation of the receptor. The array analysis evidenced the over-expression of genes involved in the phagocytic process, especially after short time of activation (Figure 27).



**Figure 27:** Heat map representing the expression of genes involved in the phagocytosis in infected macrophages upon CD300E activation. Macrophages were infected for 48 h before activating CD300E by cell exposure to the anti-CD300E agonistic monoclonal antibody (clone UP-H2, Abcam) for 3, 6 and 24 h (3 h, 6 h, or 24 h anti-CD300E). Control cells (Ctrl), infected but not activated by the antibody, were harvested at the same time points. The expression of each gene is expressed referring to the average expression of the gene considering all samples. Gene categorization (on the right) was retrieved basing the Qiagen Pathway categorization ([http://www.sabiosciences.com/rt\\_pcr\\_product/HTML/PAHS-173Z.html](http://www.sabiosciences.com/rt_pcr_product/HTML/PAHS-173Z.html)). Most of the genes are up-regulated after 3 h of CD300E activation.

The over-expression of genes involved in the phagocytosis was corroborated by the results of the phagocytosis assay, where macrophages exhibit the ability to engulf labelled particles, with a significant increase in the phagocytic activity upon CD300E activation (Figure 28).

This result could be related with the fact that the bacterium would be able to escape the clearance by surviving inside macrophages after being engulfed.

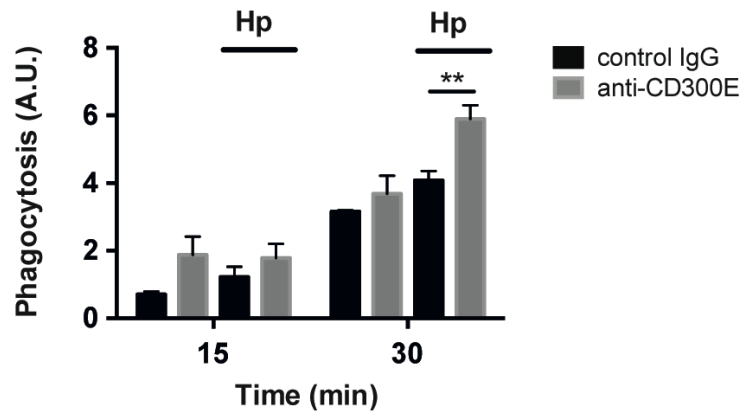


Figure 28: Impact of CD300E activation on the phagocytic process in macrophages. Three independent experiments were performed with 3 different cell preparations. Significance was determined by Student's t-test. \*\*  $p < 0.01$ .

## 5 Conclusions

Hp is still one of the most spread bacterial infections worldwide. Since it colonizes more than half of the human population and it is the major causative agent of gastric cancer, the infection by the bacterium remains a major public health issue. One of the main questions still unanswered is how the bacterium can escape the host immune surveillance leading to a long-term infection and inflammation, although an important innate and adaptive immune response is stimulated.

In this study, we focused our attention on macrophages, one of the key effector cells in innate immunity, and one of the most abundant cell types in infected gastric mucosa.

We found that Hp infection modulates the expression of several miRNAs and in particular we took in consideration those down-regulated, being permissive for inflammatory process.

Among genes up-regulated involved in inflammation we found that the main up-regulated gene was that encoding for CD300E. CD300E belongs to a protein family of immune receptors and it is mainly expressed on the plasma membrane of monocytes. Its ligand(s) are still unknown, but the engagement of this receptor by an agonistic antibody results in the expression of activation marker (CD83 and CD86) and secretion of pro-inflammatory cytokines.

Interestingly, the differentiation of monocytes into macrophages leads to a down-regulation of the expression of CD300E.

Here, we demonstrated that the infection of macrophages by Hp leads to an increased expression of CD300E through the modulation of miR-4270. Moreover, moving to an *ex vivo* model, we observed that macrophages expressing CD300E accumulated in the gastric mucosa of Hp-infected subjects with chronic gastritis while its expression significantly decreased after bacteria eradication. Notably, CD300E positive macrophages were not detectable in the gastric mucosa of Hp-negative chronic gastritis, suggesting that its up-regulation could be considered a peculiarity of Hp infection. To support this idea we also demonstrated that the exposure of macrophages to a non-pathogenic bacterium did not increase CD300E expression. To better characterize the function of this molecule in the context of Hp infection, we performed functional analysis taking advantage of the agonistic monoclonal antibody. We found that the engagement of CD300E in infected macrophages led to the release of pro-inflammatory cytokines and enhanced phagocytosis. On the contrary, we observed a reduction in the exposure of MHC-II molecules on the plasma membrane. This reduction was responsible of a reduced ability of macrophages in presenting antigens to T cells.

Based on these results, we propose the following scenario: during the first stage of infection, an adaptive immune response toward Hp is elicited; meanwhile, bacteria proliferate and impair the ability of macrophages to present the antigens, through a reduction of MHC-II expression. This would initially occur by a direct action of the bacteria on macrophages, involving a mechanism that deserves further investigation. But this effect would be reinforced by the down-regulation of miR-4270 and the subsequent up-regulation of the immune receptor CD300E. In fact, the engagement of CD300E by a ligand, which remains to be determined, would maintain the inflammatory status because of the release of cytokines, but it would also maintain the inability of macrophages to present bacterial antigens to T cells, thus impairing their local proliferation and the possibility for them to exert the effector function, such as the activation of the killing potential of macrophages through IFN- $\gamma$ .

Collectively, our results reinforce the idea that Hp-infected macrophages may have a pivotal role in the persistence of Hp in the host, not only because the normal process of phagosome maturation is altered, as already reported [89], but also because they become invisible to effector T cells, thus jeopardizing the possibility to clear the infection. Moreover, our findings contribute to understand the function of the immune receptor CD300E. Considered until now a receptor expressed on monocytes and dendritic cells, we demonstrated that it can be expressed in macrophages upon the down-modulation of miR-4270. In addition, albeit ascribed to the activating members of the CD300 family till now, it actually elicits a more articulated immune response. Considering the importance of antigen presentation, studying CD300E and identifying its ligand(s) could unravel new mechanisms of immune escape not only in chronic infectious disorders but also in diseases in which an unproductive adaptive immune response can profoundly impact their outcome.



## 6 Bibliography

1. Warren JR, Marshall B; *Unidentified curved bacilli on gastric epithelium in active chronic gastritis*. Lancet, 1983. 1(8336): p. 1273-5.
2. Maixner F, Krause-Kyora B, Turaev D, Herbig A, Hoopmann MR, Hallows JL, Kusebauch U, Egarter Vigl E, Malfertheiner P, Megraud F, O'Sullivan N, Cipollini G, Coia V, Samadelli M, Engstrand L, Linz B, Moritz RL, Grimm R, Krause J, Nebel A, Moodley Y, Rattei T, Zink A; *The 53000-year-old Helicobacter pylori genome of the Iceman*. Science, 2016. 351 (6269): p. 162-165.
3. Linz B, Balloux F, Moodley Y, Manica A, Liu H, Roumagnac P, Falush D, Stamer C, Prugnolle F, van der Merwe SW, Yamaoka Y, Graham DY, Perez-Trallero E, Wadstorm T, Suerbaum S, Achtman M; *An African origin for the intimate association between humans and Helicobacter pylori*. Nature, 2007. 445(7130): 915-918.
4. International Agency for Research on Cancer. Monographs on the evaluation of carcinogenic risks to humans. Geneva, World Health Organization (1994):61.
5. Hooi JKY, Ying Lai W, Khoo Ng W, Suen MMY, Underwood FE, Tanyingoh D, Malfertheiner P, Graham DY, Wong VWS, Wu JCY, Chan FKL, Sung JJY, Kaplan GG, Ng SC; *Global prevalence of Helicobacter pylori infection: systematic review and meta-analysis*. Gastroenterology, 2017. 153(2): p. 420-429.
6. Sitas, F., J. Yarnell, and D. Forman, *Helicobacter pylori infection rates in relation to age and social class in a population of Welsh men*. Gut, 1992. 33(11): p. 1582.
7. Parsonnet, J., H. Shmueli, and T. Haggerty, *Fecal and oral shedding of Helicobacter pylori from healthy infected adults*. JAMA, 1999. 282(23): p. 2240-5.
8. Vale, F.F. and J.M. Vitor, *Transmission pathway of Helicobacter pylori: does food play a role in rural and urban areas?* Int J Food Microbiol. 138(1-2): p. 1-12.
9. Eusebi L, Zagari RM, Bazzoli F; *Epidemiology of Helicobacter pylori infection*. Helicobacter, 2014. 19: 1-5.
10. Mobley HL, Island MD, Hausinger RP; *Molecular biology of microbial urease*. Microbiol rev, 1995. 59: 451-80
11. Scott DR, Marcus EA, Wen Y, Singh S, Feng J, Sachs G; *Cytoplasmic histidine kinase (HP0244)-regulated assembly of urease with UreI, a channel for urea and its metabolites, CO<sub>2</sub>, NH<sub>3</sub>, and NH<sub>4</sub>(+), is necessary for acid survival of Helicobacter pylori*. J Bacteriol 2010. 192: 94-103.

12. Harris PR, Mobley HL, Perez-Perez GI, Blaser MJ, Smith PD; *Helicobacter pylori* urease is a potent stimulus of mononuclear phagocyte activation and inflammatory cytokine production. *Gastroenterology*, 1996. 111(2): 419-25
13. Sfarti C, Stanciu C, Cojocariu C, Trifan A; *13C-urea breath test for the diagnosis of Helicobacter pylori infection in bleeding duodenal ulcer*. *Rev Med Chir Soc Met Nad Iasi*, 2009. 113(3): 704-9.
14. Eaton KA, Suerbaum S, Josenhans C, Krakowka S; *Colonization of gnotobiotic piglets by Helicobacter pylori deficient in two flagellin genes*. *Infect immun*, 1996. 64(7): 2445-8.
15. Lertsethtakarn P, Ottemann KM, Hendrixson DR; *Motility and chemotaxis in Campylobacter and Helicobacter*. *Annu Revv Microbiol*, 2011. 65:389-410.
16. Ilver D, Arnqvist A, Ogren J, Frick IM, Kersulyte D, Incecik ET, Berg DE, Covacci A, Engstrand L, Borén T; *Helicobacter pylori* adhesion binding fucosylated histo-blood group antigens revealed by retagging. *Science*, 1998. 279(5349): 373-7
17. Mahdavi J, Sondén B, Hurtig M, Olfat FO, Forsberg L, Roche N, Angstrom J, Larsson T, Teneberg S, Karlsson KA, Altraja S, Wadström T, Kersulyte D, Berg DE, Dubois A, Petersson C, Magnusson KE, Norberg T, Lindh F, Lundskog BB, Arnqvist A, Hammarström L, Borén T; *Helicobacter pylori SabA adhesin in persistent infection and chronic inflammation*. *Science*, 2002. 297: 573-8.
18. Rappuoli R, Lange C, Censini S, Covacci A; *Pathogenicity island mediates Helicobacter pylori interaction with the host*. *Folia microbiol (Praha)*, 1998. 43(3): 275-8.
19. Censini S, Lange C, Xiang Z, Crabtree JE, Ghiara P, Borodovsky M, Rappuoli R, Covacci A; *Cag, a pathogenicity island of Helicobacter pylori, encodes type I-specific and disease-associated virulence factors*. *Proc Natl Acad Sci USA*, 1996. 93: 14648-14653.
20. Backert S, Tegtmeyer N, Fischer W; *Composition, structure and function of the Helicobacter pylori cag pathogenicity island encoded type IV secretion system*. *Future Microbiol*, 2015. 10: 955-965.
21. Schuelein R, Everingham P, Kwok T; *Integrin-mediated type IV secretion by Helicobacter: what makes it tick?*. *Trends in Microbiology*, 2011. 19(5): 211-216.
22. Murata-Kamyra N, Kikuchi K, Hayashi T, Higashi H, Hatakeyama M; *Helicobacter pylori exploits host membrane phosphatidylserine for delivery, localization, and*

- pathophysiological action of the CagA oncoprotein*. Cell Host & Microbe, 2010. 7(5): p. 399-411.
23. Backert S, Moese S, Selbach M, Brinkmann V, Meyer TF; *Phosphorylation of tyrosine 972 of the Helicobacter pylori CagA protein is essential for induction of a scattering phenotype in gastric epithelial cells*. Molecular Microbiology, 2001. 42(3): 631-644.
24. Stein M, Bagnoli F, Halenbeck R, Rappuoli R, Fantl WJ, Covacci A; *c-Src/Lyn kinases activate Helicobacter pylori CagA through tyrosine phosphorylation of the EPIYA motif*. Molecular Microbiology, 2002. 43(4): 971-980.
25. Argent RH, Kidd M, Owen RJ, Thomas RJ, Limb MC, Atherton JC; *Determinants and consequences of different levels of CagA phosphorylation for clinical isolates of Helicobacter pylori*. Gastroenterology, 2004. 127: 514-23.
26. Higashi H, Tsutsumi R, Muto S, Sugiyama T, Azuma T, Asaka M, Hatakeyama M; *SHP-2 Tyrosine phosphatase as an intracellular target of Helicobacter pylori CagA protein*. Science, 2002. 295: 683-686.
27. Amieva MR, Vogelmann R, Covacci A, Tompkins LS, Nelson WJ, Falkow S; *Disruption of the epithelial apical-junction complex by Helicobacter pylori CagA*. Science, 2003. 300: 1430-1434.
28. Franco AT, Israel DA, Washington MK, Krishna U, Fox JG, Rogers AB, Neish AS, Collier-Hyams L, Perez-Perez GI, Hakeyama M, Whitehead R, Gaus K, O'brien DP, Romero-Gallo J, Peej Jr RM; *Activation of beta-catenin by carcinogenic Helicobacter pylori*. Proc Natl Acad Sci USA, 2005. 102: 10646-10651.
29. De Bernard M, Arico B, Papini E, Rizzuto R, Grandi G, Rappuoli R, Montecucco C; *Helicobacter pylori toxin VacA induces vacuole formation by acting in the cell cytosol*. Mol Microbiol, 1997. 26: 665-674.
30. Nguyen VQ, Caprioli RM, Cover TL; *Carboxy-terminal proteolytic processing of Helicobacter pylori vacuolating toxin*. Infect Immun, 2001. 69(1): 543-6.
31. Palframan SL, Kwok T, Gabriel K; *Vacuolating cytotoxin A (VacA), a key toxin for Helicobacter pylori pathogenesis*. Frontiers in Cellular and Infection Microbiology, 2012. 2(92): 1-9.
32. Seto K, Hayashi-Kuwabara Y, Yoneta T, Suda H, Tamaki H; *Vacuolation induced by cytotoxin from Helicobacter pylori is mediated by the EGF receptor in HeLa cells*. FEBS Lett, 1998. 431: 347-350.

33. Yahiro K, Wada A, Nakayama M, Kimura T, Ogushi K-i, Niidome T, Aoyagi H, Yoshino K-i, Yonezawa K, Moss J, Hirayama T; *Protein tyrosine phosphatase alpha, RPTP alpha, is a Helicobacter pylori VacA receptor*. J. Biol. Chem., 2003. 278: 19183-19189.
34. Roche N, Ilver D, Angstrom J, Barone S, Telford JL, Teneberg S; *Human gastric glycosphingolipids recognized by Helicobacter pylori vacuolating cytotoxin VacA*. Microbes Infect., 2007. 9: 605-614.
35. Montecucco C, de Bernard M, Papini E, Zoratti M; *Helicobacter pylori vacuolating cytotoxin: cell intoxication and anion-specific channel activity*. Curr Top Microbiol Immunol, 2001. 257: 113-29.
36. Willhite DC, Blanke SR; *Helicobacter pylori vacuolating cytotoxin enter cells, localizes to the mitochondria, and induces mitochondrial membrane permeability changes correlated to toxin channel activity*. Cell Microbiol, 2004. 6: 143-154.
37. Kimura M, Goto S, Wada A, Yahiro K, Niidome T, Hatakeyama T, Aoyagi H, Hirayama T, Kondo T; *Vacuolating cytotoxin purified from Helicobacter pylori causes mitochondrial damage in human gastric cells*. Microb Pathog, 1999. 26: 45-52.
38. Montecucco C, de Bernard M; *Immunosuppressive and proinflammatory activities of the VacA toxin of Helicobacter pylori*. J Exp Med, 2003. 198(12): 1767-71.
39. Gebert B, Fisher W, Weiss E, Hoffmann R, Haas R; *Helicobacter pylori vacuolating cytotoxin inhibits T lymphocyte activation*. Science, 2003. 301(5636): 1099-102.
40. Amedei A, Cappon A, Codolo G, Cabrelle A, Polenghi A, Benagiano M, Tasca E, Azzurri A, D'Elios MM, Del Prete G, de Bernard M; *The neutrophil-activating protein of Helicobacter pylori promotes Th1 Immune response*. J Clin Invest, 2006. 116(4): 1092-101.
41. Satin B, Del Giudice G, Della Bianca V, Dusi S, Laudanna C, Tonello F, Kelleher D, Rappuoli R, Montecucco C, Rossi F; *The neutrophil-activating protein (HP-NAP) of Helicobacter pylori is a protective antigen and a major virulence factor*. J Exp Med, 2000. 191(9): 1467-76.
42. de Bernard M, D'Elios MM; *The immune modulating activity of the Helicobacter pylori HP-NAP: friend or foe?* Toxicon, 2010. 56(7): 1186-92.
43. Li H, Liao T, Debowski AW, Tang H, Nilsson HO, Stubbs KA, Marshall BJ, Benghezal M; *Lipopolysaccharide structure and biosynthesis in Helicobacter pylori*. Helicobacter, 2016. 21: 445-461.

44. Taylor JM, Ziman ME, Huff JL, Moroski MN, Vajdy M, Solnick JV; *Helicobacter pylori* lipopolysaccharide promotes a Th1 type immune response in immunized mice. *Vaccine*, 2006. 24(23): 4987-94.
45. Bergman MP, Engering A, Smits HH, van Vliet SJ, van Bodegraven AA, Wirth HP, Kapsenberg ML, Vandenbroucke- Grauls C, van Kooyk Y, Appelmek BJ; *Helicobacter pylori* modulates the T helper cell 1/T helper cell 2 balance through phase-variable interaction between lipopolysaccharide and DC-SIGN. *J Exp Med*, 2004. 200: 979-90.
46. Parsonnet J; *The incidence of Helicobacter pylori infection*. *Aliment Pharmacol Ther*, 1995. 9 Suppl 2: 45-51.
47. Kuipers EJ; *Helicobacter pylori and the risk and management of associated diseases: gastritis, ulcer disease, atrophic gastritis and gastric cancer*. *Aliment Pharmacol Ther*, 1997. 11 Suppl 1: 71-88.
48. D'Elis MM, Bergman MP, Azzurri A, Amedei A, Benagiano M, De Pont JJ, Cianchi F, Vandenbroucke-Grauls CM, Romagnani S, Appelmek BJ, Del Prete G; *H(+),K(+)-atpase (proton pump) is the target autoantigen of Th1-type cytotoxic T cells in autoimmune gastritis*. *Gastroenterology*, 2001. 120(2): 377-86.
49. Shi Y, Liu XF, Zhuang Y, Zhang JY, Liu T, Yin Z, Wu C, Mao XH, Jia KR, Wang FJ, Guo H, Flavell RA, Zhao Z, Liu KY, Xiao B, Guo Y, Zhang WJ, Zhou WY, Guo G, Zou QM; *Helicobacter pylori-induced Th17 responses modulate Th1 cell responses, benefit bacterial grow, and contribute to pathology in mice*. *J Immunol*, 2010. 184(9): 5121-5129.
50. Zullo A, Hassan C, Cristofari F, Andriani A, De Francesco V, Ierardi E, Tomao S, Stolte M, Morini S, Vaira D; *Effects of Helicobacter pylori eradication on early stage gastric mucosa-associated lymphoid tissue lymphoma*. *Clin Gastroenterol Hepatol*, 2010. 8: 105-110.
51. Hussel T, Isaacson PG, Crabtree JE, Spencer J; *The response of cells from low-grade B-cell gastric lymphoma of mucosa-associated lymphoid tissue to Helicobacter pylori*. *Lancet*, 1993. 342(8871): 571-4.
52. Munari F, Lonardi S, Cassatella MA, Doglioni C, Cangini MG, Amedei A, Facchetti F, Eishi Y, Rugge M, Fassan M, de Bernard M, D'Elis MM, Vermi W; *Tumor-associated macrophages as major source of APRIL in gastric malt lymphoma*. *Blood*, 2011. 117(24): 6612-6.

53. Kim SS, Ruiz VE, Carroll JD, Moss SF; *Helicobacter pylori* in the pathogenesis of gastric cancer and gastric lymphoma. *Cancer Lett*, 2011. 305(2): 228-38.
54. Necchi V, Candusso ME, Tava F, Luinetti O, Ventura U, Fiocca R, Ricci V, Solcia E; *Intracellular, intercellular, and stromal invasion of gastric mucosa, preneoplastic lesions, and cancer by Helicobacter pylori*. *Gastroenterol*, 2007. 132(3): 1009-1023.
55. Montecucco C, Rappuoli R; *Living dangerously: how Helicobacter pylori survives in the human stomach*. *Nat Rev Mol Cell Biol*, 2001. 2(6): 457-66.
56. D'Elis MM, Manghetti M, De Carli M, Costa F, Baldari CT, Burrioni D, Telford JL, Romagnani S, Del Prete G; *T helper 1 effector cells specific for Helicobacter pylori in the gastric antrum of patients with peptic ulcer disease*. *J Immunol*, 1997. 158(2): 962-967.
57. Shi Y, Liu XF, Zhuang Y, Zhang JY, Liu T, Yin Z, Wu C, Mao XH, Jia KR, Wang FG, Guo H, Flavell RA, Zhao Z, Liu KY, Xiao B, Guo Y, Zhang WJ, Zhou WY, Guo G, Zou QM; *Helicobacter pylori-induced Th17 responses modulate Th1 cell responses, benefit bacterial growth, and contribute to pathology in mice*. *J Immunol*, 2010. 184(9): 5121-9.
58. Oertli M, Sundquist M, Hitzler I, Engler DB, Arnold IC, Reuter S, Maxeiner J, Hansson M, Taube C, Quinding-Järbrink M, Müller A; *DC-derived IL-18 drives Treg differentiation, murine Helicobacter pylori-specific immune tolerance, and asthma protection*. *J Clin Invest*, 2012. 122(3): 1082-96.
59. Wilson KT, Crabtree JE; *Immunology of Helicobacter pylori: insights into the failure of the immune response and perspectives on vaccine studies*. *Gastroenterol*, 2007. 133: 288-308.
60. Viladomiu M, Bassaganya-Riera J, Tubau-Juni N, Kronsteiner B, Leber A, Philipson CW, Zoccoli-Rodriguez V, Hontecillas R; *Cooperation of gastric mononuclear phagocytes with Helicobacter pylori during colonization*. *J Immunol*, 2017. 198(8): 3195-204.
61. Carbo A, Bassaganya-Riera J, Pedragosa M, Viladomiu M, Marathe M, Eubank S, Wendelsdorf K, Bisset K, Hoops S, Deng X, Alam M, Kronsteiner B, Mei Y, Hontecillas R; *Predictive computational modeling of the mucosal immune responses during Helicobacter pylori infection*. *PLoS One*, 2013. 8(9): e73365.
62. Gobert AP, McGee DJ, Akhtar M, Mendz GL, Newton JC, Cheng Y, Mobley HLT, Wilson KT; *Helicobacter pylori arginase inhibits nitric oxide production by eukaryotic cells: a strategy for bacterial survival*. *PNAS*, 2001. 98(24): 13844-13849.

63. Harris PR, Ernst PB, Kawabata S, Kiyono H, Graham MF, Smith PD; *Recombinant Helicobacter pylori urease activates primary mucosal macrophages*. J Infect Dis, 1998. 178: 1516-1520.
64. Molinari M, Salio M, Galli C, Norais N, Rappuoli R, Lanzavecchia A, Montecucco C; *Selective inhibition of Ii-dependent antigen presentation by Helicobacter pylori toxin VacA*. J Exp Med, 1998. 187(1): 135-140.
65. Tomita T, Jackson AM, Hida N, Hayat M, Dixon MF, Shimoyama T, Axon AT, Robinson PA, Crabtree JE; *Expression of interleukin-18, a Th1 cytokine, in human gastric mucosa is increased in Helicobacter pylori infection*. J Infect Dis, 2001. 183:620.
66. Salama NR, Hartung ML, Müller A; *Life in the human stomach: persistence strategies of the bacterial pathogen Helicobacter pylori*. Natute Microbiol, 2013. 11: 385-399.
67. D'Elis MM, Czinn SJ; *Immunity, inflammation, and vaccines for Helicobacter pylori*. Helicobacter, 2014. 19 Suppl 1: 19-26.
68. Rad R, Brenner L, Bauer S, Schwendy S, Layland L, da Costa CP, Reindl W, Dossumbekova A, Friedrich M, Saur D, Wagner H, Schmid RM, Prinz C; *CD25+/Foxp3+ T cells regulate gastric inflammation and Helicobacter pylori colonization in vivo*. Gastroenterol, 2006. 131: 525-537.
69. Starega-Roslan J, Koscianska E, Kozlowski P, Krzyzosiak WJ; *The role of the precursor structure in the biogenesis of microRNA*. Cell Mol Life Sci, 2011. 68: 2859-2871.
70. de la Guardia AH, Staedel C, Kaafarany I, Clement A, Roubaud Baudron C, Mégraud F, Lehours P; *Inflammatory cytokine and microRNA responses of primary human dendritic cells cultured with Helicobacter pylori strains*. Front Microbiol, 2013. 4: 1-13.
71. Kiga K, Mimuro H, Suzuki M, Shinozaki-Ushiku A, Kobayashi T, Sanada T, Kim M, Ogawa M, Iwasaki YW, Kayo H, Fukuda-Yuzawa Y, Yashiro M, Fukayama M, Fukao T, Sasakawa C; *Epigenetic silencing of mir-210 increases the proliferation of gastric epithelium during chronic Helicobacter pylori infection*. Nature Communication, 2014. 5:4497.
72. Baud J, Varon C, Chabas S, Chambonnier L, Darfeuille F, Staedel C; *Helicobacter pylori initiates a mesenchymal transition through ZEB1 in gastric epithelial cells*. Plos One, 2013. 8(4).

73. Wellner U, Schubert J, Burk UC, Schmalhofer O, Zhu F, Sonntag A, Waldvogel B, Vannier C, Darling D, zur Hausen A, Brunton VG, Morton J, Sansom O, Schüler J, Stemmler MP, Herzberger C, Hopt U, Keck T, Brabletz S, Brabletz T; *The EMT-activator ZEB1 promotes tumorigenicity by repressing stemness-inhibiting microRNAs*. Nature Cell Biol, 2009. 11(12): 1487-1504.
74. Weiss G, Forster S, Irving A, Tate M, Ferrero RL, Hertzog P, Frøkiær H, Kaparakis-Liaskos M; *Helicobacter pylori VacA suppresses Lactobacillus acidophilus-induced interferon beta signaling in macrophages via alterations in the endocytic pathway*. MBio, 2013. 4(3): e609-12.
75. Tusher VG, Tibshirani R, Chu G; *Significance analysis of microarrays applied to the ionizing radiation response*. Proc Natl Acad Sci USA, 2001. 98(9): 5116-21.
76. Kasprzyk A; *Biomart: driving a paradigm change in biological data management*. Database (Oxford), 2011. 2011:bar049.
77. Sherman BT, Huang da W, Tan Q, Guo Y, Bour S, Liu D, Stephens R, Baseler MW, Lane HC, Lempicki RA; *DAVID knowledgebase: a gene-centered database integrating heterogeneous gene annotation resources to facilitate high-throughput gene functional analysis*. BMC Bioinformatics, 2007. 8: 426.
78. Subramanian A, Tamayo P, Mootha VK, Mukherjee S, Ebert BL, Gillette MA, Paulovich A, Pomeroy SL, Golub TR, Lander ES, Mesirov JP; *Gene set enrichment analysis: a knowledge-based approach for interpreting genome-wide expression profiles*. Proc Natl Acad Sci USA, 2005. 102(43): 15545-50.
79. Mootha VK, Lindgren CM, Eriksson KF, Subramanian A, Sihag S, Lehar J, Pulgserver P, Carlsson E, Ridderstrale M, Laurila E, Houstis N, Daly MJ, Patterson N, Mesirov JP, Golub TR, Tamayo P, Spiegelman B, Lander ES, Hirschhorn JN, Altshuer D, Groop LC; *PGC-1alpha-responsive genes involved in oxidative phosphorylation are coordinately downregulated in human diabetes*. Nat Genet, 2003. 34(3): 267-73.
80. Risso D, Massa Ms, Chiogna M, Romualdi C; *A modified LOESS normalization applied to microRNA arrays: a comparative evaluation*. Bioinformatics, 2009. 25(29): 2685-91.
81. Saeed A, Sharov V, White J, Li J, Liang W, Bhagabati N, Braisted J, Klapa M, Currier T, Thiagarajan M, Sturn A, Snuffin M, Rezantsev A, Popov D, Rytsov A, Kostukovich E, Borisovsky I, Liu Z, Vinsavich A, Trush V, Quackenbush J; *TM4: a*



- free, open-source system for microarray data management and analysis*. Biotechniques, 2003. 34(2): 374-8.
82. Lu M, Shi B, Wang J, Cao Q, Cui Q; *TAM: a method for enrichment and depletion analysis of a microRNA category in a list of microRNAs*. BMC Bioinformatics, 2010. 11: 419.
83. Wang X, El Naqa IM,; *Prediction of both conserved and nonconserved microRNA targets in animals*. Bioinformatics, 2008. 24(3): 325-32.
84. Shannon P, Markiel A, Ozier O, Baliga NS, Wang JT, Ramage D, Amin N, Schwikowski B, Ideker T; *Cytoscape: a software environment for integrated models of biomolecular interaction networks*. Genome Res, 2003. 13(11): 2498-504.
85. Benagiano M, Munari F, Ciervo A, Amedei A, Paccani SR, Mancini F, Ferrari M, Della Bella C, Ulivi C, D'Elios S, Baldari CT, Prisco D, de Bernard M, D'Elios MM; *Chlamydomonas pneumonia phospholipase D (CpPLD) drives Th17 inflammation in human atherosclerosis*. Proc Natl Acad Sci USA, 2012. 109(4): 1222-7.
86. Martinez-Barriocanal A, Comas-Casellas E, Schwartz S Jr, Martin M, Sayos J; *CD300 heterocomplexes, a new and family-restricted mechanism for myeloid cell signalling regulation*. J Biol Chem, 2010. 285(53): 41781-94.
87. Aguilar H, Alvarez-Errico D, Garcia-Montero AC, Orfao A, Sayos J, Lopez-Botet M; *Molecular characterization of a novel immune receptor restricted to the monocytic lineage*. J Immunol, 2004. 173: 6703-6711.
88. Brckalo T, Calzetti F, Pérez-Cabezas B, Borràs FE, Cassatella MA, Lopez-Botet M; *Functional analysis of the CD300e receptor in human monocytes and myeloid dendritic cells*. Eur J Immunol, 2010. 40: 722-732.
89. Borlace GN, Jones HF, Keep SJ, Butler RN, Brooks DA; *Helicobacter pylori phagosome maturation in primary human macrophages*. Gut Pathog, 2011. 3(1): 3.